Title: The *trans*-zeatin-type side-chain modification of cytokinins controls rice growth

Takatoshi Kiba[1,2], Kahori Mizutani[1], Aimi Nakahara[1], Yumiko Takebayashi[2], Mikiko Kojima[2], Tokunori Hobo[3], Yuriko Osakabe[4,5], Keishi Osakabe[5], and Hitoshi Sakakibara[1,2]

1. Graduate School of Bioagricultural Sciences, Nagoya University, Furocho, Chikusa-ku, Nagoya, 464-8601, Japan
2. RIKEN Center for Sustainable Resource Science, 1-7-22, Suehiro, Tsurumi, Yokohama 230-0045, Japan
3. Biosci. Biotech Center, Nagoya University., Furocho, Chikusa-ku, Nagoya, 464-8601, Japan
4. Department of Life Science and Technology, Tokyo Institute of Technology, Yokohama, 226-8501, Japan
5. Graduate School of Technology, Industrial and Social Sciences, Tokushima University, Tokushima, 770-8503, Japan,

Corresponding Author: Takatoshi Kiba: e-mail: kiba@agr.nagoya-u.ac.jp, TEL: 81-52-789-5511; FAX: 81-52-789-4095

Running head: Roles of *trans*-zeatin-type cytokinins in rice

Abstract

Cytokinins (CKs), a class of phytohormones with vital roles in growth and development, occur naturally with various side-chain structures, including N^6-(Δ^2-isopentenyl)adenine-, *cis*-zeatin- and *trans*-zeatin (tZ)-types. Recent studies in a model dicot plant *Arabidopsis* demonstrated that tZ-type CKs are biosynthesized via cytochrome P450 monooxygenase (P450) CYP735A, and have a specific function in shoot growth promotion. Although the function of some of these CKs has been demonstrated in a few dicotyledonous plant species, the significance of these variations and their biosynthetic mechanism and function in monocots and in plants with distinctive side-chain profiles than *Arabidopsis*, such as *Oryza sativa* (rice), remain elusive. In this study, we characterized *CYP735A3* and *CYP735A4* to investigate the role of tZ-type CKs in rice. Complementation test of the *Arabidopsis* CYP735A-deficient mutant and CK profiling of loss-of-function rice mutant, *cyp735a3 cyp735a4*, demonstrated that *CYP735A3* and *CYP735A4* encode P450s required for tZ-type side-chain modification in rice. *CYP735As* are expressed in both roots and shoots. The *cyp735a3 cyp735a4* mutants exhibited growth retardation concomitant with reduction in CK activity in both roots and shoots, indicating that tZ-type CKs function in growth promotion of both organs. Expression analysis revealed that tZ-type CK biosynthesis is negatively regulated by auxin, abscisic acid, and cytokinin and positively by dual nitrogen nutrient signals, namely glutamine-related and nitrate-specific signals. These results suggest that the physiological role of tZ-type CKs in rice is different from that in *Arabidopsis* and they control growth of both roots and shoots in response to internal and environmental cues in rice.

Introduction

Cytokinins (CKs), a group of plant hormones, are involved in the regulation of various aspects of plant growth and development, including cell division and differentiation, organogenesis, root and shoot growth, and environmental responses (Mok and Mok, 2001; Sakakibara, 2006; Werner and Schmülling, 2009; Kiba et al., 2011; Kieber and Schaller, 2018; Kiba et al., 2019; Sakakibara, 2021). Natural CKs are mostly derivatives of adenine with a prenyl side chain at the N^6 position. There are variations in the side-chain structure of CKs and the most common structures in plants are N^6-(Δ^2-isopentenyl)adenine (iP)-, *trans*-zeatin (tZ)-, and *cis*-zeatin (cZ)-types, which differ in the presence and stereoisomeric position of the terminal hydroxyl group on the prenyl side chain (Shaw, 1994; Mok and Mok, 2001; Gajdošová et al., 2011).

Our understanding of biosynthetic pathways of the side-chain variants has greatly progressed, thanks mostly to studies in *Arabidopsis*. The initial step of *de novo* iP- and tZ-type CK biosynthesis is catalyzed by adenosine phosphate-isopentenyltransferase (IPT) to produce iP-type CK nucleotide precursors, iP ribotides (iPRPs) (Kakimoto, 2001; Takei et al., 2001a). tZ-type side chain is formed by the enzyme cytochrome P450 monooxygenase CYP735A, which is encoded by *CYP735A1* and *CYP735A2* in *Arabidopsis* (Takei et al., 2004; Kiba et al., 2013). CYP735A *trans*-hydroxylates the prenyl side chain of iPRPs to produce tZ ribotides (tZRPs). Finally, the cytokinin-activating enzyme LONELY GUY (LOG) converts the nucleotide precursors to their active nucleobase forms, iP and tZ (Kurakawa et al., 2007; Kuroha et al., 2009; Tokunaga et al., 2012). The cZ-type CKs are biosynthesized via the prenylation of tRNA by tRNA-isopentenyltransferase (tRNA-IPT) and the degradation of the prenylated tRNA (Miyawaki et al., 2006; Gajdošová et al., 2011).

Genes responsible for prenylated tRNA degradation for cZ-type CK production have not been identified yet.

CK biosynthesis is regulated by various internal and environmental factors (Hirose et al., 2008; Zwack and Rashotte, 2015). Nitrogen nutrition, which is available mostly as nitrate and ammonium in soil (Miller and Cramer, 2004; Kirk and Kronzucker, 2005; Xu et al., 2012; Kiba and Krapp, 2016; Coskun et al., 2017), is one of the major factors. Studies in *Arabidopsis* showed that *IPT3* and *CYP735As* are induced by a nitrate-specific signal to boost iP- and tZ-type CK accumulation in *Arabidopsis* (Miyawaki et al., 2004; Takei et al., 2004; Engelsberger and Schulze, 2012; Maeda et al., 2018). *OsIPT4* and *OsIPT5* are not induced by nitrate itself but by ammonium and glutamine with accompanying accumulation of iP-type and tZ-type CKs, indicating that *de novo* iP- and tZ-type CK biosynthesis is regulated by glutamine-related signals in rice (Kamada-Nobusada et al., 2013). A *CYP735A* gene in *Oryza longistaminata*, a wild rice, was shown to be upregulated by ammonium nitrate but the signal responsible for the upregulation is not known (Shibasaki et al., 2021). Thus, plants have dual systems, nitrate-specific and glutamine-related systems, to modulate the iP-type and tZ-type CK biosynthesis in response to nitrogen availability. Although the underlying mechanism is not understood, cZ-type CK levels are generally increased in response to biotic and abiotic stresses, such as phosphate starvation, low temperature, drought, and salt treatment (Vyroubalová et al., 2009; Macková et al., 2013; Vanková et al., 2014; Silva-Navas et al., 2019).

Previous studies have suggested that there is biological relevance to side-chain variations of CKs (Schmitz and Skoog, 1972; Mok et al., 1978; Werner et al., 2003; Spíchal et al., 2004; Gajdošová et al., 2011; Stolz et al., 2011; Choi et al., 2012;

93 Osugi and Sakakibara, 2015; Schäfer et al., 2015). However, it is only recently that
94 studies in *Arabidopsis* demonstrated it. The abundance of iP- and tZ-type CKs is higher than
95 that of cZ-type (Osugi and Sakakibara, 2015; Osugi et al., 2017; Kiba et al., 2019)
96 and tZ-type CKs are the most active, while cZ-type CKs are the least active in bioassays in
97 *Arabidopsis* (Gajdošová et al., 2011; Kudo et al., 2012). *Arabidopsis* CK receptors have
98 different affinities toward side-chain variants (Spíchal et al., 2004; Romanov et al., 2006;
99 Stolz et al., 2011). For example, AHK2 and AHK4/WOL/CRE1 have high affinity to both
100 iP and tZ, while AHK3 binds to iP with a ten times lower affinity than tZ in *in vitro* binding
101 assays. Consistent with the bioassay, the affinity of AHKs to cZ is significantly lower
102 compared with that of iP and tZ (Spíchal et al., 2004; Romanov et al., 2006; Stolz et al.,
103 2011). Furthermore, characterization of the *Arabidopsis cyp735a1 cyp735a2* mutant that is
104 impaired in tZ-type side-chain modification has unequivocally shown that the function of
105 tZ-type CKs is shoot growth promotion, and it is different from iP-type and cZ-type CKs
106 (Kiba et al., 2013). Thus, tZ-type CKs are the major active variants possessing a specific
107 function in shoot growth, while cZ-type CKs are the weakly active or inactive forms with
108 minor roles in *Arabidopsis*.

109 Although the occurrence of the three side-chain variants is ubiquitous among plants
110 (Gajdošová et al., 2011), several lines of evidence suggest that their functional
111 differentiation may not be as universal. For instance, the tZ-type CKs is not consistently more
112 abundant than the cZ-type CKs among all plants. Plants that contain higher levels of cZ-type
113 CKs than tZ-type can be found across the whole evolutionary tree of land plants (Gajdošová
114 et al., 2011). Interestingly, many crops, including pea, potato, oats, maize and rice, are
115 cZ-type-abundant plants (Gajdošová et al., 2011; Schäfer et al., 2015). Furthermore,

116 cZ-type CKs are shown to be as active as tZ-type in some bioassays, including
117 cytokinin-responsive gene expression assay in maize cultured cell (Yonekura-Sakakibara
118 et al., 2004) and seminal root growth inhibition assay in rice (Kudo et al., 2012).
119 Consistently, cytokinin receptors of maize (ZmHK1) and rice (OsHK3 and OsHK4) were
120 shown to have similar affinity toward cZ and tZ (Lomin et al., 2011; Choi et al., 2012).
121 However, the exact function of each of these variants in plants other than *Arabidopsis*,
122 including monocot and cZ-type-abundant plants, is still unknown and remains to be
123 determined.

124 Rice is a monocot plant possessing a significantly distinctive CK side-chain profile
125 from *Arabidopsis*; cZ-type CKs comprise more than 80% of total CK in various tissues
126 (Kojima et al., 2009; Kudo et al., 2012; Osugi and Sakakibara, 2015). In this study,
127 we characterized the consequence of disruption of rice *CYP735A*s (*CYP735A3* and
128 *CYP735A4*) and demonstrated that these genes are vital for tZ-type CK biosynthesis. Our
129 results also revealed that tZ-type CK biosynthesis is regulated by phytohormones and dual
130 nitrogen signals and that tZ-type CKs act to promote root and shoot growth in rice. These
131 results suggest that the physiological role of tZ-type CKs in rice is different from that in
132 *Arabidopsis* despite the fact that the biosynthetic mechanism is conserved. The function of
133 tZ-type CKs might be optimized for each plant species depending on the body plan and/or
134 growth environments.

135

136 **Results**

137 ***CYP735A3* and *CYP735A4* complement the Arabidopsis *cyp735a1 cyp735a2* mutant**

138 In *Oryza sativa* genome, *CYP735A3* and *CYP735A4* encode proteins with high

139 amino acid sequence homology to CYP735A1 and CYP735A2, which are cytochrome P450
140 monooxygenases for tZ-type CK biosynthesis in *Arabidopsis* (Fig. S1) (Hansen et al.,
141 2021). The *cyp735a1 cyp735a2* mutant (*atcypDM)* is deficient in tZ-type CKs resulting in
142 shoot growth retardation (Kiba et al. 2013). To assess whether these genes encode enzymes
143 that catalyze the same reaction as CYP735A1 and CYP735A2, we expressed them in
144 *atcypDM* under the control of cauliflower mosaic virus (CaMV) 35S promoter. Accumulation
145 of *CYP735A3* or *CYP735A4* transcripts was confirmed by quantitative RT-PCR analysis
146 (qRT-PCR) in two independent lines of transgenic plants CYP735A3-ox or CYP735A4-ox,
147 respectively (Fig. 1A). When grown on soil, all the transgenic lines developed a rosette with
148 significantly greater diameter than *atcypDM* (Fig. 1B). Both *CYP735A3* and *CYP735A4*
149 expression resulted in an increase of tZ-type CK (tZ and its conjugates) concentration with a
150 concomitant decrease of iP-type CK (iP and its conjugates) concentration compared with
151 *atcypDM*, but no significant differences in cZ-type CK (cZ and its conjugates) concentration
152 were observed (Fig. 1C, Table S1). These results demonstrate that CYP735A3 and
153 CYP735A4 catalyze the same reaction as CYP735A1 and CYP735A2, which is the
154 *trans*-hydroxylation of CK side chain to synthesize tZ-type CKs from iP-type CKs.
155
156 **The spatial expression pattern of *CYP735A3* and *CYP735A4***
157 Expression levels of *CYP735A3* and *CYP735A4* were analyzed by qRT-PCR in
158 various organs of rice in seedling to early reproductive phases (Fig. 2). At seedling phase,
159 transcripts of *CYP735A*s were detected both in roots and shoots but they were more abundant
160 in roots as reported previously (Tsai et al., 2012) (Fig. 2A). In later phases tested, the
161 accumulation of the *CYP735A3* transcript was the highest around the vegetative shoot apex,

while that of *CYP735A4* transcript was prominent in the leaf blade of plants at vegetative and early reproductive phases (Fig. 2B).

In order to localize *CYP735A*s expression at the tissue level, we used GUS staining technique. For this purpose, we generated transgenic plants harboring a fusion of the 3.6 kb *CYP735A* upstream sequence and the *GUS* reporter gene (proCYP735A3:GUS and proCYP735A4:GUS). Similar staining patterns were observed in multiple independent T1 lines of proCYP735A3:GUS (Figs. 2C-E). However, no staining was detected in any of the proCYP735A4:GUS lines (data not shown), suggesting that the 3.6 kb upstream sequence of *CYP735A4* was not sufficient to drive expression. Consistent with the qRT-PCR results (Fig. 2A), staining was detected both in roots and shoots of proCYP735A3:GUS seedlings (Fig. 2C). The GUS activity was restricted to the vascular bundle (Fig. 2D) and observation of cross-sections revealed that the staining was pronounced in vascular parenchyma cells in the shoot, and vascular parenchyma and pericycle cells in the root (Fig. 2E).

CYP735A3 and _CYP735A4_ play a central role in tZ-type cytokinin biosynthesis in rice

To examine the role of *CYP735A*s in CK side-chain modification in rice, we disrupted *CYP735A3* and *CYP735A4* by CRISPR-Cas9 system. Two transfer RNA-based-multiplex CRISPR-Cas9 vectors, each harboring three different guides targeting unique sequences of *CYP735A3* and *CYP735A4,* were used to edit *CYP735A3* and *CYP735A4* (Figs. S2 and S3). Two independent lines with mutations in both *CYP735A3* and *CYP735A4* were identified. In a T1 line, the *cyp735a3-1* and *cyp735a4-1* alleles were found as homozygote and heterozygote, respectively (Fig. S2). In another T1 line, the *cyp735a3-2* and *cyp735a4-2* alleles were found as heterozygote and homozygote, respectively (Fig. S3). The

185 *cyp735a3-1* single, *cyp735a4-2* single, *cyp735a3-1 cyp735a4-1* (*a3a4-1*) double and
186 *cyp735a3-2 cyp735a4-2* (*a3a4-2*) double mutants were isolated from progenies of these lines.
187 The *cyp735a3-1* and *cyp735a3-2* are one-base insertions that shift the reading frame and yield
188 predicted proteins with no similarity to any Non-redundant UniProtKB/SwissProt sequences
189 and without the cytochrome P450 domain (Fig. S4). The *cyp735a4-1* and *cyp735a4-2* mutants
190 are 263- and 298-base deletions, respectively. The 263- and 298-base deletions resulted in a
191 predicted protein lacking "A helix", a secondary structure conserved among cytochrome P450s
192 (Midlik et al., 2021), and an in-frame stop codon at 4 codons after the mutation, respectively
193 (Fig. S5). Since the proteins predicted to be produced in all the mutants (except for
194 *cyp735a4-1*) are apparently inactive as cytochrome P450, we concluded that *cyp735a3-1*,
195 *cyp735a3-2*, and *cyp735a4-2* are null alleles.

196 CK concentrations in roots and shoots were measured in wild type (WT) strain
197 Nipponbare (NB), vector control (VC), and mutant strains *cyp735a3-1*, *cyp735a4-2*, *a3a4-1*
198 and *a3a4-2* seedlings grown in hydroponic culture (Fig. 3, Tables S2 and S3). The
199 concentrations of tZ-type CK and iP-type CK were comparable to WT in *cyp735a3-1* (Fig. 3A).
200 In contrast, *cyp735a4-2* had slightly decreased tZ-type CK and slightly increased iP-type CK
201 concentrations in roots and shoots as compared to the WT (Fig. 3B). In *a3a4-1* and *a3a4-2,* the
202 concentration of tZ-type CKs reduced dramatically to 3.5 to 8.8% of the wild-type levels in
203 roots and shoots, while that of iP-type CK increased more than 2 -fold. In the root of double
204 mutants, iP-type CK levels were increased so dramatically that the loss of tZ-type CK was
205 compensated in terms of the sum of iP- and tZ-type CKs (iP-/tZ-type CK quantity). On the
206 other hand, in the shoot, iP-type CK levels were increased but the iP-/tZ-type CK quantity
207 was significantly lower compared with WT (Fig. 3; Tables S2 and S3). The cZ-type CK levels

were not altered in any of the mutants (Fig. 3, Tables S2 and S3). Since the CK profiles of *a3a4-1* and *a3a4-2* are distorted in a similar manner, *cyp735a4-1* seems to be a null allele. These results show that tZ-type CKs are mostly synthesized by CYP735A3 and CYP735A4 in rice.

Disruption of *CYP735A3* and *CYP735A4* retards growth of rice

To explore the physiological role of tZ-type CKs in rice, we examined the growth and development of *cyp735a* single and double mutants from seedling phase to maturation phases. Although *cyp735a3-1* and *cyp735a4-2* single mutants were indistinguishable from control plants (WT and VC) on our growth conditions, similar significant alterations in growth and development were observed in *a3a4-1* and *a3a4-2* double mutants (Figs. 4, 5 and S6).

The double mutant seedlings showed a decrease in the length and fresh weight of the shoot and root compared with control (Figs. 4A, 4B, S6A, S6B). To determine the cause of the decrease in shoot length and fresh weight, leaf number and leaf size were measured (Figs. 4C-E). Leaf number of double mutant seedlings at 15 days after germination was reduced compared to control (Fig. 4C), indicating that the rate of leaf formation is slower in the double mutant. Leaf blade and sheath length of fully expanded third leaf was similar for the double mutant and control (Fig. 4D), while leaf blade width was decreased in the double mutant (Fig. 4E). These results indicated that a decrease in leaf number accounts for the reduction in shoot length and a decrease in leaf number and leaf width contributes to the reduction in shoot fresh weight. Reduced shoot length phenotype of the double mutant continued into later vegetative growth stage (Figs. S6C and S6D), but it cannot be attributed only to a decrease in leaf number because leaf size, namely blade length, blade width and

231 sheath length, was significantly reduced at this stage as observed in fully expanded ninth leaf
232 (Fig. 4F). In addition, the double mutant developed significantly fewer tillers compared with
233 control (Figs. 4G and 5C), suggesting that the activities of shoot apical and axillary meristems
234 are impaired.

235 All control plants headed about 83 days after germination (n=19) but double mutant
236 plants either died without heading from the main stem (16 out of 24 plants) or showed
237 delayed heading (8 out of 24 plants) (Figs. 5A and 5B). Panicle length, panicle weight and
238 number of primary panicle branch were all significantly reduced in the double mutant
239 compared to the control (Figs. 5D-G), suggesting that inflorescence meristem activity is
240 reduced. The double mutant set few but viable seeds, indicating that reproductive organ
241 development is not severely affected. Together, these results suggest that the tZ-type CKs
242 regulate both root and shoot growth, most possibly through controlling meristem activity.

243

244 **The cytokinin activity is reduced both in roots and shoots of the *cyp735a3 cyp735a4***
245 **mutant**

246 The growth defects observed in *a3a4* double mutant are reminiscent of those
247 observed in rice mutants with diminished CK activities such as type-A *RESPONSE*
248 *REGULATOR* (*RR*) *OsRR6* overexpressing lines (Hirose et al., 2007), type-B *RR* triple
249 mutant *rr21/22/23* (Worthen et al., 2019) and cytokinin receptor double mutant *hk5 hk6*
250 (Burr et al., 2021). To examine whether the CK activity is reduced in the double mutant, we
251 analyzed the expression levels of immediate-early CK-inducible type-A *RR*s by qRT-PCR
252 (Fig. 6). The expression level of all tested type-A *RR*s, except for that of *OsRR1* in roots, was
253 significantly lower in the mutants compared with WT in both roots and shoots (Figs. 6A and

254 6B). On the other hand, the expression of non-CK-inducible type-B *RR*s, *OsRR21* and
255 *OsRR23*, was not reduced (Figs. 6C and 6D). Thus, cytokinin activity in roots and shoots of
256 *a3a4* is diminished, suggesting that the *a3a4* growth phenotype is caused by decreased CK
257 activity.
258
259 **Regulation of *CYP735A3* and *CYP735A4* expression by phytohormones**
260 To obtain insights into the physiological relevance of tZ-type CK biosynthesis in rice,
261 we analyzed the responses of *CYP735A*s to phytohormones. In *Arabidopsis*, the expression of
262 *CYP735A1* and *CYP735A2* was shown to be upregulated by CK and downregulated by auxin
263 and abscisic acid (Takei et al., 2004). Tsai et al (2012) analyzed the effect of these
264 phytohormones on *CYP735A3* and *CYP735A4* expression by the NanoString nCounter system
265 but could not detect *CYP735A3* under some conditions using this system. To fully characterize
266 the response of *CYP735A*s to these phytohormones in rice, we analyzed their expression in
267 roots by qRT-PCR. Nipponbare seedings treated with phytohormones were used for the
268 analysis. *OsRR4*/*OsRR6* (Kudo et al., 2012; Tsai et al., 2012), *OsSIPP2C1* (Li et al.,
269 2013) and *OsGH3.2* (Du et al., 2012) were used as positive controls for CK, IAA and ABA
270 responses, respectively. Consistent with the NanoString analysis (Tsai et al., 2012), we found
271 that the *CYP735A4* transcript was decreased by CK (iP and tZ), IAA and ABA (Fig. 7). Our
272 qRT-PCR analysis showed that *CYP735A3* is also downregulated by CK, IAA and ABA (Fig.
273 7). Thus, rice *CYP735A*s and *Arabidopsis CYP735A*s are regulated similarly by IAA and ABA,
274 but differently by CK.
275
276 **Regulation of *CYP735A3* and *CYP735A4* expression by nitrogen sources**

277 Nitrogen nutrition is one of the major environmental factors regulating CK
278 biosynthesis, including tZ-type CK biosynthesis, for plant growth optimization (Takei et al.,
279 2001b; Kamada-Nobusada et al., 2013; Ohashi et al., 2017; Osugi et al., 2017;
280 Maeda et al., 2018; Sakakibara, 2021; Shibasaki et al., 2021; Kawai et al., 2022).
281 In *Arabidopsis*, *CYP735As* are upregulated by the nitrate-specific signal and play a crucial role
282 in nitrate-induced accumulation of tZ-type CKs (Engelsberger and Schulze, 2012; Maeda
283 et al., 2018). To test whether *CYP735A*s of rice are nitrogen-inducible, we analyzed the
284 expression levels of *CYP735A*s in roots supplemented with ammonium or nitrate (Fig. 8).
285 *OsIPT4* and *OsNIA1* were used as indicators for glutamine-related and nitrate-specific
286 responses, respectively (Kamada-Nobusada et al., 2013). *CYP735A3* was induced by both
287 ammonium and nitrate in a manner similar to *OsIPT4*, while the expression of *CYP735A4* was
288 upregulated only by nitrate like *OsNIA1* (Fig. 8A). To clarify whether *CYP735A*s are regulated
289 by glutamine-related and/or nitrate-specific signal, we examined the effect of methionine
290 sulfoximine (MSX), an inhibitor of glutamine synthetase (Fig. 8B) (Lam et al., 1996). MSX
291 pre-treatment inhibited the nitrate-triggered induction of *CYP735A3* but did not affect
292 *CYP735A4*. On the other hand, *CYP735A3* was upregulated by glutamine supplement in the
293 presence of MSX, while *CYP735A4* was not. These responses of *CYP735A3* and *CYP735A4*
294 to nitrogen sources and MSX are similar to those of *OsIPT4* and *OsNIA1*, respectively,
295 indicating that *CYP735A3* and *CYP735A4* are regulated by glutamine-related and
296 nitrate-specific signals, respectively. Together, these results suggested that tZ-type CK
297 biosynthesis in rice is controlled by dual nitrogen signals, which is different from that in
298 *Arabidopsis*.
299

Discussion

Angiosperms can be divided into four main categories in terms of their CK side-chain profile and number of cotyledons; iP/tZ-type-abundant dicot, cZ-type-abundant dicot, iP/tZ-type-abundant monocot and cZ-type-abundant monocot (Gajdošová et al., 2011). The function of some of these CKs has been demonstrated in a few dicotyledonous plant species. For example, in *Arabidopsis*, an iP/tZ-type-abundant dicot plant, CYP735As catalyze the biosynthesis of tZ-type CKs, which plays a specific role in shoot growth promotion (Kiba et al., 2013). Recently, it was suggested that CYP735A plays a similar role in *Jatropha curcas,* which is also an iP/tZ-type-abundant dicot plant (Cai et al., 2018). However, the function of CYP735A and tZ-type CKs in plants in other categories remains unknown. Here, we investigated the biosynthetic mechanism and function of tZ-type CKs in cZ-type-abundant monocot plant rice. Characterization of the *a3a4* double mutant demonstrated that *CYP735A*s play a central role in tZ-type CK biosynthesis in rice as in the iP/tZ-type-abundant dicot plants but that the physiological function of tZ-type CKs in rice is not the same as that in *Arabidopsis*, providing new insights into the biological significance of side-chain variations in plants.

Arabidopsis CYP735As catalyze the *trans*-hydroxylation of iP-type CKs to form tZ-type CKs (Takei et al., 2004; Kiba et al., 2013). Complementation test of *atcypDM* and CK quantification of *a3a4* demonstrated that CYP735A3 and CYP735A4 are the functional orthologs of *Arabidopsis* CYP735As (Figs. 1 and 3; Tables S1 to S3). The tZ-type CKs in *a3a4* was scarce but it did not completely disappear (Fig. 3; Tables S2 and S3). This is similar to what has been observed in the CYP735A-null mutants (*atcypDM*) of *Arabidopsis* and *J. curcas* (Kiba et al., 2013; Cai et al., 2018), suggesting the existence of minor

323 alternative pathway(s) in both iP/tZ-type-abundant and cZ-type-abundant plants. The
324 isomerization of cZ-type CKs is a possible pathway because *cis*-to-*trans* isomerization
325 activity has been detected in various plants, including rice (Bassil et al., 1993; Gajdošová
326 et al., 2011; Kudo et al., 2012). Although the isomerization pathway might be important
327 under certain biological contexts, given that the pathway is minor even in the
328 cZ-type-abundant rice, and that *CYP735A* homologs are found in all angiosperms whose
329 genome is completely sequenced (Hansen et al., 2021), the CYP735A pathway seems to be
330 the predominant pathway for tZ-type CK biosynthesis in angiosperms.

331 The *a3a4* mutants displayed severe growth retardation in vegetative and maturation
332 phases (Figs 4, 5, and S5). We concluded that this phenotype is the result of diminished CK
333 activity caused by a reduction in tZ-type CKs based on the following reasons: (i) the double
334 mutant had severely reduced level of tZ-type CKs (Fig. 3; Tables S2 and S3); (ii) the cytokinin
335 activity, measured by expression levels of immediate-early CK-inducible *RR* genes, was
336 reduced in the double mutant (Fig. 6); (iii) The phenotypes of the double mutant is partly
337 similar to those observed in rice mutants with severely reduced CK activity, such as *OsRR6*
338 overexpressors (Hirose et al., 2007), *rr21/22/23* (Worthen et al., 2019) and *hk5 hk6*
339 (Burr et al., 2021); (iv) our results were similar to the positive role of tZ-type CKs in rice
340 growth suggested through the analysis of OsABCG18, a transporter involved in root-to-shoot
341 CK translocation (Zhao et al., 2019); (v) similar conclusion was drawn from the data
342 obtained from equivalent experiments on *CYP735A1* and *CYP735A2* in *Arabidopsis* (Kiba et
343 al., 2013).

344 The cZ-type CKs are the dominant variants in terms of quantity comprising more
345 than 80% of total CK in various rice tissues and are suggested to be an active CK that plays a

346 role in normal growth and development in rice (Kojima et al., 2009; Choi et al., 2012;
347 Kudo et al., 2012; Osugi and Sakakibara, 2015). Our CK quantification results showed
348 that the levels of any of the cZ-type CK derivatives were not consistently altered in *a3a4* (Fig
349 3; Tables S2 and S3), indicating that cZ-type CKs are not directly relevant to the *a3a4*
350 phenotype. The iP-type CKs are also considered to be an important variant in rice because of
351 the identification of a receptor (OsHK6) with preferential affinity for iP (Choi et al., 2012).
352 In *a3a4*, the iP-type CK levels were increased to compensate for the loss of tZ-type CK in the
353 root but not sufficiently increased in the shoot (Fig. 3; Tables S2 and S3). From these results it
354 could be interpreted that the cause of the *a3a4* phenotype is an alteration in CK side-chain
355 profile (CK quality) but not CK quantity in the root and alteration in both CK quality and/or
356 quantity in the shoot. Together, our results suggest that the function of tZ-type CKs is
357 different from that of iP-type and cZ-type CKs at least in rice roots.

358 The phenotypes of *a3a4* were observed both in roots and shoots, including reduced
359 root proliferation, delayed plastochron and decreased leaf size, panicle size and tiller number
360 (Figs. 4, 5 and S5), indicating the extensive role of tZ-type CKs as growth enhancers in
361 various organs in rice. Although it is difficult to simply compare the phenotypes of *a3a4* with
362 those of *atcypDM* because monocot and dicot have remarkably different body plan, the major
363 difference lies in the existence of phenotype in the root. The *a3a4* displayed reduced
364 cytokinin activity and proliferation in the root (Figs. 4, 6 and S5), while no apparent
365 difference was detected in *atcypDM* root (Kiba et al., 2013), suggesting that the role of
366 tZ-type CKs in rice varies from that in *Arabidopsis*. The shoot specific-function of tZ-type
367 CKs in *Arabidopsis* is partly explained by the ligand preference of cytokinin receptors
368 (Spíchal et al., 2004; Romanov et al., 2006; Stolz et al., 2011; Kiba et al., 2013).

369 Among the five genes encoding cytokinin receptors (OsHK3-6, CHARK) in rice, so far, the
370 ligand preference of OsHK3, OsHK4 and OsHK6 has been investigated (Choi et al., 2012).
371 However, no receptor with preferential affinity for tZ-type CKs has been identified and the
372 mechanism underlying the functional specificity of tZ-type CKs in rice remains to be
373 elucidated.

374 Consistent with the functional distinction of tZ-type CKs between rice and
375 *Arabidopsis*, we also showed differences in responses to some internal and external cues of
376 *CYP735A*s (Figs. 2, 7 and 8). Rice *CYP735A*s are repressed by CKs (Tsai et al. 2012), while
377 *Arabidopsis CYP735A*s are induced (Takei et al., 2004), suggesting that rice and
378 *Arabidopsis* have negative feedback and positive feedback regulation, respectively, on tZ-type
379 CK function. The expression level of *CYP735A4* is high in leaves (Fig. 2) but that of
380 *Arabidopsis CYP735A*s is not (Takei et al., 2004; Kiba et al., 2013). Responses of these
381 genes to nitrogen supplement were also found to be different. *CYP735A3* and *CYP735A4* are
382 upregulated by glutamine-related and nitrate-specific signals, respectively, in rice (Fig. 8)
383 while *CYP735A*s of *Arabidopsis* are induced only by nitrate-specific signal (Engelsberger
384 and Schulze, 2012; Maeda et al., 2018). Although ammonium is known to be the major
385 form of inorganic nitrogen source in paddy field, rice utilizes not only ammonium but also
386 nitrate generated by nitrification on the root surface as inorganic nitrogen sources (Kirk and
387 Kronzucker, 2005; Yan et al., 2011). For *Arabidopsis*, which grows on aerobic soil, nitrate
388 is the major inorganic nitrogen source (Nacry et al., 2013), indicating that *CYP735As* of
389 rice and *Arabidopsis* respond to nitrogen in a way relevant to the nitrogen source availability
390 of the plants. Nitrogen-dependent tZ-type CK accumulation has been proposed to be involved
391 in growth enhancement in response to nitrogen supply in various plants (Takei et al.,

392 2001b; Kamada-Nobusada et al., 2013; Ohashi et al., 2017; Maeda et al., 2018;
393 Sakakibara, 2021; Shibasaki et al., 2021). Thus, the dual nitrogen-signal-dependent
394 upregulation of tZ-type CK biosynthesis might play a similar role in rice. Consistent to that,
395 there are reports suggesting that rice grows better with simultaneous supply of nitrate and
396 ammonium than exclusive supply of nitrate or ammonium (Chanch and Ohira, 1982;
397 Ying-Hua et al., 2006). Together, these differences between rice and *Arabidopsis* might be the
398 result of evolution and/or domestication to optimize growth depending on their body plan and
399 growth environments, though further investigation into the physiological function of tZ-type
400 CKs in other plant species is necessary to clarify this issue.
401
402 **Materials and Methods**
403 **Plant material and growth conditions**
404 *Arabidopsis thaliana* ecotype Columbia (Col-0) was used as the wild type. The
405 *cyp735a1-2 cyp735a2-2* double mutant was characterized previously (Kiba et al., 2013).
406 *Arabidopsis* plants were grown on half-strength Murashige-Skoog (1/2x MS) agar plates (1%
407 agar and 1% sucrose) placed vertically or on soil (Supermix A, Sakata, Japan) at 22°C under
408 fluorescent light (100 μmol m^{-2} s^{-1}, 16 h light/8 h dark).
409 *Oryza sativa* cultivar Nipponbare (NB) was used as the wild type. Rice seeds were
410 germinated on moist filter paper at 30°C for 2-3 days in the dark and then grown under
411 hydroponic culture or soil culture conditions. For hydroponic culture, germinated seeds were
412 sown on mesh trays floating on the nutrient solution (Makino et al., 1985) with or without
413 nitrogen source (NH_4NO_3 was replaced with KCl) and grown in an environment-controlled
414 greenhouse at 28°C with a 15-h light (500 μmol m^{-2} s^{-1})/9-h dark cycle. The nutrient solution

415 was renewed every 3-4 days. To analyze *CYP735A3* and *CYP735A4* expression in response to
416 nitrogen, 12-day-old seedlings grown on the nutrient solution without nitrogen source were
417 incubated with the nutrient solution without nitrogen source supplemented with KCl, NH_4Cl,
418 KNO_3, or methionine sulfoximine (MSX). For soil culture, germinated seeds were sown on a
419 synthetic soil (SunAgro, No. 3) and grown in an environment-controlled greenhouse at 28°C
420 with a 15-h light (500 μmol m^{-2} s^{-1})/9- h dark cycle. Fifteen-day-old seedlings were
421 transplanted in perforated plastic pots (10 × 12 × 15 cm) filled with nutrient-free soil (Aichi
422 Medel) supplemented with slow-release fertilizer (N, P, and K at 0.3, 0.3, and 0.3 g/kg soil,
423 respectively) and grown in a greenhouse at Nagoya University with supplemental lighting
424 (13-h light/11-h dark cycle).
425
426 **Generation of transgenic lines overexpressing *CYP735A3* or *CYP735A4* in *cyp735a1***
427 ***cyp735a2***
428 The *CYP735A3* and *CYP735A4* cDNA were amplified with the specific primer sets
429 oxCYP735A3-F/R and oxCYP735A4-F/R, respectively (Table S4). The amplified fragments
430 were cloned into the *Xba* I/*Sac* I site of pBI121 (Clontech) located downstream of the
431 cauliflower mosaic virus (CaMV) 35S promoter and introduced into *cyp735a1-2 cyp735a2-2*
432 double mutant by floral-dipping (Clough and Bent, 1998).
433
434 **CRISPR-Cas9 mutagenesis of *CYP735A3* and *CYP735A4***
435 The mutants of *CYP735A3* and *CYP735A4* were generated using the transfer
436 RNA-based-multiplex CRISPR-Cas9 vector, pMgPoef4_129-2A-GFP (Toda et al., 2019).
437 Guide sequences for *CYP735A3* and *CYP735A4* were designed by CHOPCHOP (Labun et al.,

438 2019) and two multiplex CRISPR-Cas9 vectors pMg129_A3A4-1 and pMg129_A3A4-2,
439 each harboring three guide sequences for *CYP735A3* and *CYP735A4* sequences, were
440 constructed as described (Toda et al., 2019). pMg129_A3A4-1 and pMg129_A3A4-2
441 contained guide sequences g3-1, g4-1-1, and g4-1-2 (Fig. S1), and g3-2, g4-1-2, and g4-1-2
442 (Fig. S2), respectively. Transgenic rice plants were generated by the *Agrobacterium*
443 *tumefaciens*-mediated method (Hirose et al., 2005) using EHA105 strain harboring the
444 vectors. Mutations were identified by DNA sequencing of PCR products amplified with
445 specific primer sets, gCYP735A3-F2/R2 and gCYP735A4-F3R3 (Table S4), and genomic
446 DNA prepared from T1 plants. A T1 line transformed using pMg129_A3A4-2 but without any
447 mutations in *CYP735A3* and *CYP735A* was used as the vector control line. For assays,
448 *cyp735a3-1*, *cyp735a4-2*, *cyp735a3-1 cyp735a4-1*, *cyp735a3-2 cyp735a4-2* and vector control
449 identified by genotyping progenies of these lines were used.
450
451 **Quantification of plant hormones**
452 Cytokinin levels were determined as described previously (Kojima et al., 2009;
453 Kojima and Sakakibara, 2012) using an ultra-performance liquid chromatograph coupled
454 with a tandem quadrupole mass spectrometer (ACQUITY UPLC™ System/XEVO-TQS;
455 Waters, Milford, MA, USA) with an octadecylsilyl (ODS) column (ACQUITY UPLC HSS
456 T3, 1.8 μm, 2.1 mm × 100 mm, Waters). In the results, iP, iP-riboside, iP-riboside
457 5'-phosphates, iP-7-*N*-glucoside, and iP-9-*N*-glucoside are collectively referred to as "iP-type
458 cytokinin"; tZ, tZ-riboside, tZ-riboside 5'-phosphates, tZ-7-*N*-glucoside, tZ-9-*N*-glucoside,
459 tZ-*O*-glucoside, and tZR-*O*-glucoside are collectively referred to as "tZ-type cytokinin"; cZ,

460 cZ-riboside, cZ-riboside 5'-phosphates, cZ-*O*-glucoside, and cZR-*O*-glucoside are
461 collectively referred to as "cZ-type cytokinin".
462
463 **Gene expression analysis**
464 Total RNA was extracted from root and shoot samples using the RNeasy Plant Mini
465 kit (QIAGEN) in combination with the RNase-Free DNase set (QIAGEN). Total RNA was
466 used for first strand cDNA synthesis by the ReverTra Ace qPCR RT Master Mix (Toyobo).
467 Quantitative reverse transcription-PCR (qRT-PCR) was performed on a Quant Studio 3
468 Real-Time PCR system (Thermo Fisher) with the KAPA SYBR Fast qPCR kit (KAPA
469 Biosystems). *ZIURP1* (LOC_Os03g08010/Os03g0234200) was used as an internal control
470 because this gene has been shown to be one of the most stably expressed genes in rice
471 (Pabuayon et al., 2016). Primer sets are listed in Table S4.
472
473 **Promoter-GUS analysis**
474 The *CYP735A3* promoter (proCYP735A3; -3636 to +21 bp relative to the inferred initiation
475 codon) and *CYP735A4* promoter (proCYP735A4; -3623 to +21 bp) were amplified with
476 PrimeSTAR GXL DNA polymerase (Takara) and the specific primer sets proCYP735A3-F/R
477 and proCYP735A4-F/R, respectively (Table S4). The fragments were cloned into
478 pENTR/D-TOPO vector (Thermo Fisher), sequenced, and then integrated into the GATEWAY
479 binary vector pCAMBIA-GW-GUS (Kudo et al., 2012) to generate
480 pCAMBIA1390-proCYP735A3:GUS and pCAMBIA1390-proCYP735A4:GUS vectors.
481 Transgenic rice plants were generated by the *Agrobacterium tumefaciens*-mediated method
482 (Hirose et al., 2005) using EHA105 strain harbouring the vectors. Histochemical analysis of

483 GUS activity was conducted as described previously (Hirose et al., 2005; Kiba et al.,
484 2018). Fresh and GUS-stained samples were fixed and then embedded in Technovit 7100 resin
485 (Heraeus Kulzer) as instructed by the manufacturer. Sections were produced using a Leica
486 RM2165 microtome (Leica) and observed under an Olympus BX51 microscope (Olympus).
487

488 **Morphological analyses**

489 The rosette diameter, shoot length, root length, leaf blade length, leaf sheath length,
490 leaf width, panicle length, and culm length were measured manually or determined from
491 pictures using ImageJ (https://imagej.nih.gov/ij/). The days leading to the appearance of a
492 panicle in main stem is defined as "days to heading".
493

494 **Treatment with phytohormones and nitrogen sources**

495 For phytohormone treatments, 12-day-old Nipponbare seedlings grown in hydroponic
496 culture with the nutrient solution (Makino et al., 1985) containing 1 mM NH_4NO_3 were
497 used. Phytohormone stock solutions were prepared by dissolving N^6-(Δ^2-isopentenyl)adenine
498 (iP), *trans*-zeatin (tZ), indole-3-acetic acid (IAA), and abscisic acid (ABA) in dimethyl
499 sulfoxide (DMSO) at 100 mM and added to the nutrient solution. Roots of the seedlings were
500 submerged in the nutrient solution containing 1 μM iP, 1 μM tZ, 10 μM IAA, 50 μM ABA,
501 0.001% DMSO (mock for iP and tZ treatment), or 0.05% DMSO (mock for IAA and ABA
502 treatment) and harvested after 2 h.

503 For nitrogen treatments, Nipponbare seedlings were grown in hydroponic culture
504 with the nitrogen-free nutrient solution (1 mM NH_4NO_3 was replaced with 1 mM KCl) for 12
505 days. Roots of the seedlings were incubated with the nitrogen-free nutrient solution

506 supplemented with 5 mM KCl, 5 mM NH_4Cl, or 5 mM KNO_3 for 2 h or 4 h. In case of MSX
507 and nitrogen co-treatment, roots were pre-treated with the nitrogen-free nutrient solution
508 containing 2 mM MSX for 2 h and then incubated with the MSX containing nitrogen-free
509 nutrient solution supplemented with 5 mM KCl, 5 mM KNO_3 or 50 mM glutamine for 2 h.
510

511 **Statistical analysis**

512 Data are shown as means ± standard deviation (SD) of one representative
513 experiment. In order to examine whether hormone concentration, gene expression, or
514 morphological data were significantly different between treatments, Student's *t*-test, and
515 Tukey's honestly significant difference (HSD) test were performed using KaleidaGraph ver.
516 4.1 software (Synergy Software).
517

518 **Accession numbers**

519 Sequence data for the genes described in this article can be found in The
520 Arabidopsis Information Resource database (http://www.arabidopsis.org) and Oryzabase
521 (https://shigen.nig.ac.jp/rice/oryzabase/) under the following accession numbers: *CYP735A1*
522 (At5g38450), *CYP735A2* (At1g67110), *ACT8* (AT1G49240), *CYP735A3*
523 (LOC_Os08g33300/Os08g0429800), *CYP735A4* (LOC_Os09g23820/Os09g0403300),
524 *ZIURP1* (LOC_Os03g08010/Os03g0234200), *OsRR1* (LOC_Os04g36070/Os04g0442300),
525 *OsRR2* (LOC_Os02g35180/Os02g0557800), *OsRR4* (LOC_Os01g72330/Os01g0952500),
526 *OsRR6* (LOC_Os04g57720/Os04g0673300), *OsRR9* (LOC_Os11g04720/Os11g0143300),
527 *OsRR10* (LOC_Os12g04500/Os12g0139400), *OsRR21* (LOC_Os03g12350/Os03g0224200),
528 *OsRR23* (LOC_Os02g55320/Os02g0796500), *OsSIPP2C1*

(LOC_Os09g15670/Os09g0325700), *OsGH3.2* (LOC_Os01g55940/Os01g0764800), *OsIPT4* (LOC_Os03g59570/Os03g0810100), *OsNIA1* (LOC_Os08g36480/Os08g0468100).

Acknowledgments

This work was supported by JSPS KAKENHI (No. JP18H04793 and JP20H02888 for T.K., JP17H06473 for H.S.).

Author contributions

T.K. and H.S. designed the experiments; T.K., K.M., A.M., Y.T., M.K., T.H., Y.O., K.O., H.S. performed the experiments, T.K., K.M., A.M. analyzed the data, and T.K. and H.S. wrote the paper.

References

Bassil N V, Mok D, Mok MC (1993) Partial purification of a cis-trans-isomerase of zeatin from immature seed of *Phaseolus vulgaris* L. Plant Physiol **102**: 867–872

Burr CA, Sun J, Yamburenko M V., Willoughby A, Hodgens C, Boeshore SL, Elmore A, Atkinson J, Nimchuk ZL, Bishopp A, et al (2021) The HK5 and HK6 cytokinin receptors mediate diverse developmental pathways in rice. Development **147**: dev191734

Cai L, Zhang L, Fu Q, Xu ZF (2018) Identification and expression analysis of cytokinin metabolic genes IPTs, CYP735A and CKXs in the biofuel plant *Jatropha curca*s. PeerJ **2018**: e4812

Chanch T, Ohira K (1982) Comparison of the uptake and assimilation of ammonium and nitrate in indica and japonica rice plants using the tracer 15N method. Soil Sci Plant Nutr **28**: 79–90

Choi J, Lee J, Kim K, Cho M, Ryu H, An G, Hwang I (2012) Functional identification of OsHk6 as a homotypic cytokinin receptor in rice with preferential affinity for iP. Plant Cell Physiol **53**: 1334–1343

Clough SJ, Bent AF (1998) Floral dip: a simplified method for Agrobacterium-mediated

557 transformation of Arabidopsis thaliana. Plant J **16**: 735–743
558 **Coskun D, Britto DT, Shi W, Kronzucker HJ** (2017) Nitrogen transformations in modern
559 agriculture and the role of biological nitrification inhibition. Nat Plants **3**: 17074
560 **Du H, Wu N, Fu J, Wang S, Li X, Xiao J, Xiong L** (2012) A GH3 family member,
561 OsGH3-2, modulates auxin and abscisic acid levels and differentially affects drought and
562 cold tolerance in rice. J Exp Bot **63**: 6467–6480
563 **Engelsberger WR, Schulze WX** (2012) Nitrate and ammonium lead to distinct global
564 dynamic phosphorylation patterns when resupplied to nitrogen-starved Arabidopsis
565 seedlings. Plant J **69**: 978–995
566 **Gajdošová S, Spíchal L, Kamínek M, Hoyerová K, Novák O, Dobrev PI, Galuszka P,**
567 **Klíma P, Gaudinová A, Žižková E, et al** (2011) Distribution, biological activities,
568 metabolism, and the conceivable function of *cis*-zeatin-type cytokinins in plants. J Exp
569 Bot **62**: 2827–2840
570 **Hansen CC, Nelson DR, Møller BL, Werck-Reichhart D** (2021) Plant cytochrome P450
571 plasticity and evolution. Mol Plant **14**: 1244–1265
572 **Hirose N, Makita N, Kojima M, Kamada-Nobusada T, Sakakibara H** (2007)
573 Overexpression of a type-A response regulator alters rice morphology and cytokinin
574 metabolism. Plant Cell Physiol **48**: 523–539
575 **Hirose N, Makita N, Yamaya T, Sakakibara H** (2005) Functional characterization and
576 expression analysis of a gene, OsENT2, encoding an equilibrative nucleoside transporter
577 in rice suggest a function in cytokinin transport. Plant Physiol **138**: 196–206
578 **Hirose N, Takei K, Kuroha T, Kamada-Nobusada T, Hayashi H, Sakakibara H** (2008)
579 Regulation of cytokinin biosynthesis, compartmentalization and translocation. J Exp Bot
580 **59**: 75–83
581 **Kakimoto T** (2001) Identification of plant cytokinin biosynthetic enzymes as dimethylallyl
582 diphosphate : ATP/ADP isopentenyltransferases. Plant Cell Physiol **42**: 677–685
583 **Kamada-Nobusada T, Makita N, Kojima M, Sakakibara H** (2013) Nitrogen-dependent
584 regulation of *de novo* cytokinin biosynthesis in rice: the role of glutamine metabolism as
585 an additional signal. Plant Cell Physiol **54**: 1881–1893
586 **Kawai M, Tabata R, Ohashi M, Honda H, Kamiya T, Kojima M, Takebayashi Y, Oishi S,**
587 **Okamoto S, Hachiya T, et al** (2022) Regulation of ammonium acquisition and use in
588 *Oryza longistaminata* ramets under nitrogen source heterogeneity. Plant Physiol **188**:
589 2364–2376
590 **Kiba T, Inaba J, Kudo T, Ueda N, Konishi M, Mitsuda N, Takiguchi Y, Kondou Y,**
591 **Yoshizumi T, Ohme-Takagi M, et al** (2018) Repression of nitrogen-starvation

592 responses by members of the Arabidopsis GARP-type transcription factor NIGT1/HRS1
593 subfamily. Plant Cell **30**: 925–945
594 **Kiba T, Kudo T, Kojima M, Sakakibara H** (2011) Hormonal control of nitrogen
595 acquisition: roles of auxin, abscisic acid, and cytokinin. J Exp Bot **62**: 1399–1409
596 **Kiba T, Takebayashi Y, Kojima M, Sakakibara H** (2019) Sugar-induced *de novo* cytokinin
597 biosynthesis contributes to Arabidopsis growth under elevated CO_2. Sci Rep **9**: 1–15
598 **Kiba T, Takei K, Kojima M, Sakakibara H** (2013) Side-chain modification of cytokinins
599 controls shoot growth in *Arabidopsis*. Dev Cell **27**: 452–461
600 **Kieber JJ, Schaller GE** (2018) Cytokinin signaling in plant development. Development **145**:
601 dev149344
602 **Kirk GJ, Kronzucker HJ** (2005) The potential for nitrification and nitrate uptake in the
603 rhizosphere of wetland plants: a modelling study. Ann Bot **96**: 639–646
604 **Kojima M, Kamada-Nobusada T, Komatsu H, Takei K, Kuroha T, Mizutani M, Ashikari**
605 **M, Ueguchi-Tanaka M, Matsuoka M, Suzuki K, et al** (2009) Highly sensitive and
606 high-throughput analysis of plant hormones using MS-probe modification and liquid
607 chromatography tandem mass spectrometry: an application for hormone profiling in
608 *Oryza sativa*. Plant Cell Physiol **50**: 1201–1214
609 **Kojima M, Sakakibara H** (2012) Highly sensitive high-throughput profiling of six
610 phytohormones using MS-probe modification and liquid chromatography-tandem mass
611 spectrometry. Methods Mol Biol **918**: 151–164
612 **Kudo T, Makita N, Kojima M, Tokunaga H, Sakakibara H** (2012) Cytokinin activity of
613 *cis*-zeatin and phenotypic alterations induced by overexpression of putative
614 *cis*-Zeatin-*O*-glucosyltransferase in rice. Plant Physiol **160**: 319–331
615 **Kurakawa T, Ueda N, Maekawa M, Kobayashi K, Kojima M, Nagato Y, Sakakibara H,**
616 **Kyozuka J** (2007) Direct control of shoot meristem activity by a cytokinin-activating
617 enzyme. Nature **445**: 652–655
618 **Kuroha T, Tokunaga H, Kojima M, Ueda N, Ishida T, Nagawa S, Fukuda H, Sugimoto K,**
619 **Sakakibara H** (2009) Functional analyses of LONELY GUY cytokinin-activating
620 enzymes reveal the importance of the direct activation pathway in *Arabidopsis*. Plant
621 Cell **21**: 3152–3169
622 **Labun K, Montague TG, Krause M, Torres Cleuren YN, Tjeldnes H, Valen E** (2019)
623 CHOPCHOP v3: Expanding the CRISPR web toolbox beyond genome editing. Nucleic
624 Acids Res **47**: W171–W174
625 **Lam HM, Coschigano KT, Oliveira IC, Melo-Oliveira R, Coruzzi GM** (1996) The
626 molecular-genetics of nitrogen assimilation into amino acids in higher plants. Annu Rev

Plant Physiol Plant Mol Biol **47**: 569–593

Li YS, Sun H, Wang ZF, Duan M, Huang SD, Yang J, Huang J, Zhang HS (2013) A novel nuclear protein phosphatase 2C negatively regulated by ABL1 is involved in abiotic stress and panicle development in rice. Mol Biotechnol **54**: 703–710

Lomin SN, Yonekura-Sakakibara K, Romanov GA, Sakakibara H (2011) Ligand-binding properties and subcellular localization of maize cytokinin receptors. J Exp Bot **62**: 5149–5159

Macková H, Hronková M, Dobrá J, Turečková V, Novák O, Lubovská Z, Motyka V, Haisel D, Hájek T, Prášil IT, et al (2013) Enhanced drought and heat stress tolerance of tobacco plants with ectopically enhanced cytokinin oxidase/dehydrogenase gene expression. J Exp Bot **64**: 2805–2815

Maeda Y, Konishi M, Kiba T, Sakuraba Y, Sawaki N, Kurai T, Ueda Y, Sakakibara H, Yanagisawa S (2018) A NIGT1-centred transcriptional cascade regulates nitrate signalling and incorporates phosphorus starvation signals in *Arabidopsis*. Nat Commun **9**: 1–14

Makino A, Mae T, Ohira K (1985) Photosynthesis and ribulose-1,5-bisphosphate carboxylase oxygenase in rice leaves from emergence through senescence - quantitative-analysis by carboxylation oxygenation and regeneration of ribulose 1,5-bisphosphate. Planta **166**: 414–420

Midlik A, Navrátilová V, Moturu TR, Koča J, Svobodová R, Berka K (2021) Uncovering of cytochrome P450 anatomy by SecStrAnnotator. Sci Rep **11**: 12345

Miyawaki K, Matsumoto-Kitano M, Kakimoto T (2004) Expression of cytokinin biosynthetic isopentenyltransferase genes in *Arabidopsis*: tissue specificity and regulation by auxin, cytokinin, and nitrate. Plant J **37**: 128–138

Miyawaki K, Tarkowski P, Matsumoto-Kitano M, Kato T, Sato S, Tarkowska D, Tabata S, Sandberg G, Kakimoto T (2006) Roles of Arabidopsis ATP/ADP isopentenyltransferases and tRNA isopentenyltransferases in cytokinin biosynthesis. Proc Natl Acad Sci USA **103**: 16598–16603

Mok DW, Mok MC (2001) Cytokinin metabolism and action. Annu Rev Plant Physiol Plant Mol Biol **52**: 89–118

Mok MC, Mok DW, Armstrong DJ (1978) Differential cytokinin structure-activity relationships in Phaseolus. Plant Physiol **61**: 72–75

Nacry P, Bouguyon E, Gojon A (2013) Nitrogen acquisition by roots: physiological and developmental mechanisms ensuring plant adaptation to a fluctuating resource. Plant Soil **370**: 1–29

662 **Ohashi M, Ishiyama K, Kojima S, Kojima M, Sakakibara H, Yamaya T, Hayakawa T**
663 (2017) Lack of cytosolic glutamine synthetase1;2 activity reduces nitrogen-dependent
664 biosynthesis of cytokinin required for axillary bud outgrowth in rice seedlings. Plant Cell
665 Physiol **58**: 679–690
666 **Osugi A, Kojima M, Takebayashi Y, Ueda N, Kiba T, Sakakibara H** (2017) Systemic
667 transport of *trans*-zeatin and its precursor have differing roles in Arabidopsis shoots. Nat
668 Plants **3**: 1–6
669 **Osugi A, Sakakibara H** (2015) Q&A: How do plants respond to cytokinins and what is their
670 importance? BMC Biol **13**: 102
671 **Pabuayon IM, Yamamoto N, Trinidad JL, Longkumer T, Raorane ML, Kohli A** (2016)
672 Reference genes for accurate gene expression analyses across different tissues,
673 developmental stages and genotypes in rice for drought tolerance. Rice **9**: 32
674 **Romanov GA, Lomin SN, Schmülling T** (2006) Biochemical characteristics and
675 ligand-binding properties of Arabidopsis cytokinin receptor AHK3 compared to
676 CRE1/AHK4 as revealed by a direct binding assay. J Exp Bot **57**: 4051–4058
677 **Sakakibara H** (2006) Cytokinins: activity, biosynthesis, and translocation. Annu Rev Plant
678 Biol **57**: 431–449
679 **Sakakibara H** (2021) Cytokinin biosynthesis and transport for systemic nitrogen signaling.
680 Plant J **105**: 421–430
681 **Schäfer M, Brütting C, Meza-Canales ID, Großkinsky DK, Vankova R, Baldwin IT,**
682 **Meldau S** (2015) The role of cis-zeatin-type cytokinins in plant growth regulation and
683 mediating responses to environmental interactions. J Exp Bot. Oxford University Press,
684 pp 4873–4884
685 **Schmitz RY, Skoog F** (1972) Cytokinins: Synthesis and biological activity of geometric and
686 position isomers of zeatin. Plant Physiol **50**: 702–705
687 **Shaw G** (1994) Chemistry of adenine cytokinins. *In* DWS Mok, MC Mok, eds, Cytokinins:
688 Chemistry, Activity, and Function. CRC Press, Boca Rato, FL, pp 15–34
689 **Shibasaki K, Takebayashi A, Makita N, Kojima M, Takebayashi Y, Kawai M, Hachiya T,**
690 **Sakakibara H** (2021) Nitrogen nutrition promotes rhizome bud outgrowth via
691 regulation of cytokinin biosynthesis genes and an *Oryza longistaminata* ortholog of
692 *FINE CULM 1*. Front Plant Sci **12**: 788
693 **Spíchal L, Rakova NY, Riefler M, Mizuno T, Romanov GA, Strnad M, Schmülling T**
694 (2004) Two cytokinin receptors of *Arabidopsis thaliana*, CRE1/AHK4 and AHK3, differ
695 in their ligand specificity in a bacterial assay. Plant Cell Physiol **45**: 1299–1305
696 **Stolz A, Riefler M, Lomin SN, Achazi K, Romanov GA, Schmülling T** (2011) The

specificity of cytokinin signalling in *Arabidopsis thaliana* is mediated by differing ligand affinities and expression profiles of the receptors. Plant J **67**: 157–168

Takei K, Sakakibara H, Sugiyama T (2001a) Identification of genes encoding adenylate isopentenyltransferase, a cytokinin biosynthesis enzyme, in *Arabidopsis thaliana*. J Biol Chem **276**: 26405–26410

Takei K, Sakakibara H, Taniguchi M, Sugiyama T (2001b) Nitrogen-dependent accumulation of cytokinins in root and the translocation to leaf: implication of cytokinin species that induces gene expression of maize response regulator. Plant Cell Physiol **42**: 85–93

Takei K, Yamaya T, Sakakibara H (2004) Arabidopsis CYP735A1 and CYP735A2 encode cytokinin hydroxylases that catalyze the biosynthesis of *trans*-zeatin. J Biol Chem **279**: 41866–41872

Toda E, Koiso N, Takebayashi A, Ichikawa M, Kiba T, Osakabe K, Osakabe Y, Sakakibara H, Kato N, Okamoto T (2019) An efficient DNA- and selectable-marker-free genome-editing system using zygotes in rice. Nat Plants **5**: 363–368

Tokunaga H, Kojima M, Kuroha T, Ishida T, Sugimoto K, Kiba T, Sakakibara H (2012) Arabidopsis lonely guy (LOG) multiple mutants reveal a central role of the LOG-dependent pathway in cytokinin activation. Plant J **69**: 355–365

Tsai Y-C, Weir NR, Hill K, Zhang W, Kim HJ, Shiu S-H, Schaller GE, Kieber JJ (2012) Characterization of Genes Involved in Cytokinin Signaling and Metabolism from Rice. Plant Physiol **158**: 1666–1684

Vanková R, Kosová K, Dobrev P, Vítámvás P, Trávníčková A, Cvikrová M, Pešek B, Gaudinová A, Prerostová S, Musilová J, et al (2014) Dynamics of cold acclimation and complex phytohormone responses in *Triticum monococcum* lines G3116 and DV92 differing in vernalization and frost tolerance level. Environ Exp Bot **101**: 12–25

Vyroubalová S, Václavíková K, Turečková V, Novák O, Šmehilová M, Hluska T, Ohnoutková L, Frébort I, Galuszka P (2009) Characterization of new maize genes putatively involved in cytokinin metabolism and their expression during osmotic stress in relation to cytokinin levels. Plant Physiol **151**: 433–447

Werner T, Motyka V, Laucou V, Smets R, Van Onckelen H, Schmülling T (2003) Cytokinin-deficient transgenic Arabidopsis plants show multiple developmental alterations indicating opposite functions of cytokinins in the regulation of shoot and root meristem activity. Plant Cell **15**: 2532–2550

Werner T, Schmülling T (2009) Cytokinin action in plant development. Curr Opin Plant Biol

12: 527–538

Worthen JM, Yamburenko M V, Lim J, Nimchuk ZL, Kieber JJ, Schaller GE (2019) Type-B response regulators of rice play key roles in growth, development and cytokinin signaling. Development **146**: dev174870

Xu GH, Fan XR, Miller AJ (2012) Plant nitrogen assimilation and use efficiency. Annu Rev Plant Biol **63**: 153–182

Yan M, Fan XR, Feng HM, Miller AJ, Shen QR, Xu GH (2011) Rice OsNAR2.1 interacts with OsNRT2.1, OsNRT2.2 and OsNRT2.3a nitrate transporters to provide uptake over high and low concentration ranges. Plant Cell Environ **34**: 1360–1372

Yonekura-Sakakibara K, Kojima M, Yamaya T, Sakakibara H (2004) Molecular characterization of cytokinin-responsive histidine kinases in maize. differential ligand preferences and ¥response to cis-zeatin. Plant Physiol **134**: 1654–1661

Zhao J, Yu N, Ju M, Fan B, Zhang Y, Zhu E, Zhang M, Zhang K (2019) ABC transporter OsABCG18 controls the shootward transport of cytokinins and grain yield in rice. J Exp Bot **70**: 6277–6291

Zwack PJ, Rashotte AM (2015) Interactions between cytokinin signalling and abiotic stress responses. J Exp Bot **66**: 4863–4871

Legends to Figures

Figure 1. Recovery of *trans*-zeatin-type cytokinin deficiency in the *Arabidopsis* mutant *cyp735a1 cyp735a2* by *CYP735A3* or *CYP735A4*

(A) Quantitative RT-PCR analysis of *CYP735A3* (left) or *CYP735A4* (right) expression in whole seedlings of Col-0, *cyp735a1 cyp735a2* mutant (*atcypDM*), and transgenic plants constitutively expressing *CYP735A3* (*A3*-ox) or *CYP735A4* (*A4*-ox) in *atcypDM* background. Seedlings were grown on 1/2x MS agar plates for 12 days before harvest. Expression levels were normalized using *ACT8* as an internal control. Error bars represent standard deviation (n=4 independent pools of more than ten plants). N.D., under the quantification detection limit. (B) Rosette diameter of 28-day-old Col-0, *atcypDM,* and transgenic plants constitutively expressing *CYP735A3* (*A3*-ox) or *CYP735A4* (*A4*-ox) in *atcypDM* background

761 grown on soil. A photograph of representative plants is shown. Error bars represent standard
762 deviation (n=7). Asterisks indicate statistically significant differences compared with
763 *atcypDM* (p<0.01, Student's t-test). Scale bar, 3 cm. (C) Cytokinin concentrations in whole
764 seedlings of Col-0, *atcypDM* and transgenic plants constitutively expressing *CYP735A3*
765 (*A3*-ox) or *CYP735A4* (*A4*-ox) in *atcypDM* background. Seedlings were grown on 1/2x MS
766 agar plates for 12 days before harvest. Error bars represent standard deviation (n=4
767 independent pools of more than ten plants). Asterisks indicate statistically significant
768 differences in tZ-type cytokinin concentration compared with *atcypDM* (p<0.01, Student's
769 t-test). The concentration of each cytokinin molecular species in roots and shoots is shown in
770 Table S1. gFW, gram fresh weight; tZ-type, *trans*-zeatin and its conjugates; cZ-type,
771 *cis*-zeatin and its conjugates; iP-type, N^6-(Δ^2-isopentenyl)adenine and its conjugates.
772
773 **Figure 2. Expression pattern of *CYP735A3* and *CYP735A4* in various tissues**
774 (A) Expression of *CYP735A3* and *CYP735A4* in Nipponbare seedlings. Coleoptiles and
775 seminal roots, and roots and shoots were harvested 4 days and 14 days, respectively, after
776 imbibition. Error bars represent standard deviation of biological replicates (n=4-5 independent
777 pools of more than 2 plants). (B) Expression of *CYP735A3* and *CYP735A4* in Nipponbare
778 plants in vegetative or early reproductive stages. 42-day-old (vegetative stage) and older
779 plants (reproductive stage) were used. The shoot apex parts of 42-day-old plants were
780 collected as shoot apical meristem (SAM). Leaf blade, leaf sheath and lamina joint were
781 harvested from the youngest fully expanded leaf. The young panicle is a mixture of 2 mm to
782 21 mm long young panicles collected from plants at the reproductive stage. Error bars
783 represent standard deviation of biological replicates (n=4 except for SAM and young panicle,

n=4 and n=7 independent pools of more than 2 plants for SAM and young panicle, respectively). N.D., under the quantification detection limit. (C-E) Representative images of GUS staining obtained from *proCYP735A3:GUS* transgenic seedlings grown for 8 days after imbibition. Pictures of a whole seedling (C), first leaf (D, upper), crown root (D, lower), cross section of the first leaf (E, upper), and cross section of seminal root (E, lower) are presented. VBS, vascular bundle sheath; XY, xylem; PH, phloem; EN, endodermis; PE, pericycle. Scale bars, (C) 1 cm; (D) 200 μm; (E) 50 μm.

Figure 3. The *cyp735a3 cyp735a4* double mutants show deficiency in *trans*-zeatin-type cytokinins

Cytokinin concentrations in roots and shoots of WT strain Nipponbare (NB), vector control (VC), and mutant strains *cyp735a3-1* (*a3-1*), *cyp735a4-2* (*a4-2*), *cyp735a3-1 cyp735a4-1* (*a3a4-1*), and *cyp735a3-2 cyp735a4-2* (*a3a4-2*). Seedlings were grown hydroponically for 14 days (A) or 12 days (B) before shoots and roots were harvested. Error bars represent standard deviation of biological replicates (n=3-6 independent pools of more than ten plants for A, n=6-8 independent pools of more than ten plants for B). Asterisks indicate statistically significant differences in tZ-type cytokinin concentration compared with NB ($p<0.05$, Student's *t*-test). The concentration of each cytokinin molecular species in roots and shoots is shown in Table S2 and Table S3. gFW, gram fresh weight; tZ-type, *trans*-zeatin and its conjugates; cZ-type, *cis*-zeatin and its conjugates; iP-type, N^6-(Δ^2-isopentenyl)adenine and its conjugates.

Figure 4. Disruption of *CYP735A*s alters rice growth in seedling to vegetative phases

807 (A) A representative image of Nipponbare (NB), vector control (VC), and *cyp735a3-2*
808 *cyp735a4-2* (*a3a4-2*) seedlings grown 12 days in hydroponic culture. Scale bar, 5 cm. (B)
809 Quantification of shoot length, shoot fresh weight, root length, and root fresh weight in
810 12-day-old seedlings. NB, VC, *cyp735a4-2* (*a4-2*), and *a3a4-2* seedlings were grown in
811 hydroponic culture. (C) Leaf number at 15 days after germination (D, E) Leaf sheath and leaf
812 blade length (D) and leaf width (E) of the fully expanded third leaf of NB, VC, *cyp735a3-1*
813 (*a3-1*), *cyp735a4-2* (*a4-2*), *cyp735a3-1 cyp735a4-1* (*a3a4-1*), and *a3a4-2* seedlings grown on
814 soil. (F) Quantification of leaf blade length, leaf sheath length, and leaf width of the fully
815 expanded ninth leaf in NB, VC, *a3a4-1*, and *a3a4-2* grown on soil. (G) Tiller number of NB,
816 VC, *a3a4-1*, and *a3a4-2* grown on soil for 35 days. Error bars represent standard deviation of
817 biological replicates (B, n=6-8; C, n=8-12; D, n=8-10; E, n=8-10; F, n=8-12; G, n=4-8).
818 Different lowercase letters indicate statistically significant differences as indicated by Tukey's
819 HSD test (p<0.05).
820
821 **Figure 5. Disruption of *CYP735A*s alters rice growth in reproductive to maturation**
822 **phases**
823 (A) A representative image of Nipponbare (NB), vector control (VC), and *cyp735a3-1* (*a3-1*),
824 *cyp735a4-1* (*a4-2*), and *cyp735a3-1 cyp735a4-1* (*a3a4-2*) plants grown 15 weeks on soil.
825 Scale bar, 20 cm. (B-D) Heading date (B), panicle and culm length (C), and tiller number (D)
826 of NB, VC, *a3-1*, *a4-2*, *cyp735a3-1 cyp735a4-1* (*a3a4-1*), and *a3a4-2*. (E) A representative
827 picture of mature panicles from NB and *a3a4-2*. Scale bar, 5 cm. (F, G) Panicle weight on the
828 main stem (F) and number of primary branches per panicle (G). Error bars represent standard
829 deviation of biological replicates (B, n=3-12; C, n=5-12; D, n=9-12; F, n=5-10; G, n=5-10).

830 Different lowercase letters indicate statistically significant differences as indicated by Tukey's
831 HSD test (p<0.05).
832
833 **Figure 6. Expression of cytokinin inducible type-A response regulator genes is altered in**
834 **the *cyp735a3 cyp735a4* mutant**
835 (A, B) Transcript levels of cytokinin inducible type-A response regulator genes, *OsRR1*,
836 *OsRR2*, *OsRR*4, *OsRR6*, and *OsRR9/10*, in shoots (A) and roots (B) of Nipponbare (NB),
837 vector control (VC), *cyp735a3-1 cyp735a4-1* (*a3a4-1*) and *cyp735a3-2 cyp735a4-2* (*a3a4-2*)
838 seedlings. *OsRR9/10* indicates that the primer set used could not distinguish *OsRR9* and
839 *OsRR10*. (C, D) Transcript levels of type-B response regulator genes, *OsRR21* and *OsRR23*,
840 in the shoot. (C) and in the root (D) of NB, VC, *a3a4-1* and *a3a4-2* seedlings. Seedlings were
841 grown hydroponically for 10 days before roots and shoots were harvested. Expression levels
842 were quantified by qRT-PCR analysis, normalized to *ZIURP1* as an internal control, and are
843 shown relative to the value of NB. Error bars represent standard deviation of biological
844 replicates (n=4 independent pools of 2 plants). Asterisks indicate statistically significant
845 differences compared to NB (p<0.05, Student's t-test).
846
847 **Figure 7. Expression of *CYP735A3* and *CYP735A4* in response to phytohormones**
848 (A) Expression of *CYP735A*s in response to cytokinin. Nipponbare (NB) seedlings grown for
849 12 days were treated with 0.001% DMSO (Mock), 1 μM iP (iP), or 1 μM tZ (tZ) and roots
850 were harvested after 2 h. (B) Expression of *CYP735A*s in response to abscisic acid (ABA) and
851 auxin. NB seedlings grown for 12 days were treated with 0.05% DMSO (Mock), 10 μM
852 indole-3-acetic acid (IAA) or 50 μM ABA and roots were harvested after 2 h. Expression

853 levels were quantified by qRT-PCR analysis, normalized to *ZIURP1* as an internal control,
854 and are shown relative to the value in mock treatment. Asterisks indicate statistically
855 significant differences compared with Mock (p<0.05, Student's t-test). Error bars represent
856 standard deviation (n=4 independent pools of more than 2 plants).
857
858 **Figure 8. Expression of *CYP735A3* and *CYP735A4* in response to nitrogen sources**
859 (A) Expression of *CYP735A*s in response to ammonium or nitrate supplement.
860 Twelve-day-old NB seedlings hydroponically grown in nitrogen-free nutrient solution were
861 incubated with 5 mM KCl (-N), 5 mM NH_4Cl (NH_4^+), or 5 mM KNO_3 (NO_3^-) for 2 h or 4 h.
862 Expression levels were quantified by qRT-PCR analysis, normalized to *ZIURP1* as an internal
863 control, and are shown relative to the value in 2 h of -N treatment. Error bars represent
864 standard deviation (n=4 independent pools of 3 plants). (B) Effect of methionine sulfoximine
865 on the induction of *CYP735A*s by nitrogen. Twelve-day-old NB seedlings hydroponically
866 grown in nitrogen-free nutrient solution were pre-treated with 2 mM MSX for 2 h and then
867 incubated with 5 mM KCl, 5 mM KNO_3 or 50 mM glutamine (GLN) for 2 h. Asterisks
868 indicate statistically significant differences compared with KCl or KCl+MSX (p<0.05,
869 Student's t-test). Expression levels were quantified by qRT-PCR analysis, normalized to
870 *ZIURP1* as an internal control, and are shown relative to the value in KCl treatment. Error
871 bars represent standard deviation (n=4 independent pools of 3 plants).
872
873 **Supplemental Figure 1. Phylogenetic tree of *Arabidopsis* cytochrome P450s, CYP735A3**
874 **and CYP735A4**
875 (A) A phylogenetic tree of 293 *Arabidopsis* P450s, CYP735A3

(LOC_Os08g33300/Os08g0429800) and CYP735A4 (LOC_Os09g23820/Os09g0403300). (B) Enlargement of a subclade with CYP735A3 and CYP735A4. Full-length amino acid sequences were obtained from Plant P450 database (https://erda.dk/public/vgrid/PlantP450/index.html). A phylogenetic tree was inferred by the Neighbour-Joining method using MEGAX (https://www.megasoftware.net/). The tree is drawn to scale, with branch lengths in the same units as those of the evolutionary distances used to infer the phylogenetic tree. The evolutionary distances were computed using the JTT matrix-based method and are in the units of the number of amino acid substitutions per site. All positions containing gaps and missing data were eliminated. The values at the nodes indicate the bootstrap values (using 500 replications).

Supplemental Figure 2. The *cyp735a3-1 cyp735a4-1* mutant generated by the CRISPR/Cas9 system

(A) Schematic representation of CRISPR target sites to generate *cyp735a3-1* (*a3-1*) and *cyp735a4-1* (*a4-1*) alleles. Boxes represent exons; horizontal bars, introns; triangles, CRISPR target sites. The blue box represents the “A helix”. The bar indicates a 200 bp scale. (B) Partial sequences of wild-type *CYP735A3* and *cyp735a3-1* (*a3-1*) mutant. The sequence corresponding to a guide RNA used to generate the *a3-1* mutation (g3-1) is highlighted in yellow. (C) Partial sequences of wild-type *CYP735A4* and *cyp735a4-1* (*a4-1*) mutant. The sequence corresponding to guide RNAs used to generate the *a4-1* mutation (g4-1-1 and g4-1-2) is highlighted in yellow. Numbers in (B) and (C) represent positions in a genome sequence when the first nucleotide of the putative start codon is counted as 1. The red letter and red dash indicate an inserted and deleted sequence, respectively.

Supplemental Figure 3. The *cyp735a3-2 cyp735a4-2* mutant generated by CRISPR/Cas9 system

(A) Schematic representation of CRISPR target sites to generate *cyp735a3-2* (*a3-2*) and *cyp735a4-2* (*a4-2*) alleles. Boxes represent exons; horizontal bars, introns; triangles, CRISPR target sites. The blue box represents the "A helix". The bar indicates a 200 bp scale. (B) Partial sequences of wild-type *CYP735A3* and *cyp735a3-2* (*a3-2*) mutant. The sequence corresponding to a guide RNA used to generate the *a3-2* mutation (g3-2) is highlighted in yellow. (C) Partial sequences of wild-type *CYP735A4* and *cyp735a4-2* (*a4-2*) mutant. The sequence corresponding to guide RNAs used to generate the *a4-2* mutation (g4-2-1 and g4-2-2) is highlighted in green. Numbers in (B) and (C) represent positions in a genome sequence when the first nucleotide of the putative start codon is counted as 1. The red letter and red dash indicate an inserted and deleted sequence, respectively.

Supplemental Figure 4. Deduced amino acid sequences of *CYP735A3*, *cyp735a3-1* and *cyp735a3-2*

Deduced amino acid sequences of *CYP735A3*, *cyp735a3-1* (*a3-1*), and *cyp735a3-2* (*a3-2*) were aligned by Clustal Omega (https://www.ebi.ac.uk/Tools/msa/clustalo/). Triangles indicate CRISPR target sites.

Supplemental Figure 5. Deduced amino acid sequences of *CYP735A4*, *cyp735a4-1* and *cyp735a4-2*

Deduced amino acid sequences of *CYP735A4*, *cyp735a4-1* (*a4-1*), and *cyp735a4-2* (*a4-2*)

922 were aligned by Clustal Omega (https://www.ebi.ac.uk/Tools/msa/clustalo/). Triangles
923 indicate CRISPR target sites. The "A helix" is highlighted in blue.
924
925 **Supplemental Figure 6. Effect of disruption of *CYP735A*s on vegetative growth**
926 (A) A representative image of Nipponbare (NB), vector control (VC), *cyp735a3-1 cyp735a4-1*
927 (*a3a4-1*), and *cyp735a3-1* (*a3-1*) seedlings grown 14 days in hydroponic culture. Scale bar, 5
928 cm. (B) Quantification of shoot length, shoot fresh weight, root length, and root fresh weight
929 of 14-day-old seedlings. NB, VC, *cyp735a3-1* (*a3-1*), and *a3a4-1* seedlings were grown in
930 hydroponic culture. (C) A representative image of NB, VC, *a3-1*, *cyp735a4-1* (*a4-2*),
931 *cyp735a3-2 cyp735a4-2* (*a3a4-2*) seedlings grown for 43 days on soil. Scale bar, 20 cm. (D)
932 Plant height and leaf number of NB, VC, *a3-1*, *a4-2*, *a3a4-1*, and *cyp735a3-2 cyp735a4-2*
933 (*a3a4-2*) grown for 30 days on soil. Error bars represent standard deviation of biological
934 replicates (B, n=6-13; D, n=9-12). Different lowercase letters indicate statistically significant
935 differences as indicated by Tukey's HSD test ($p<0.05$).

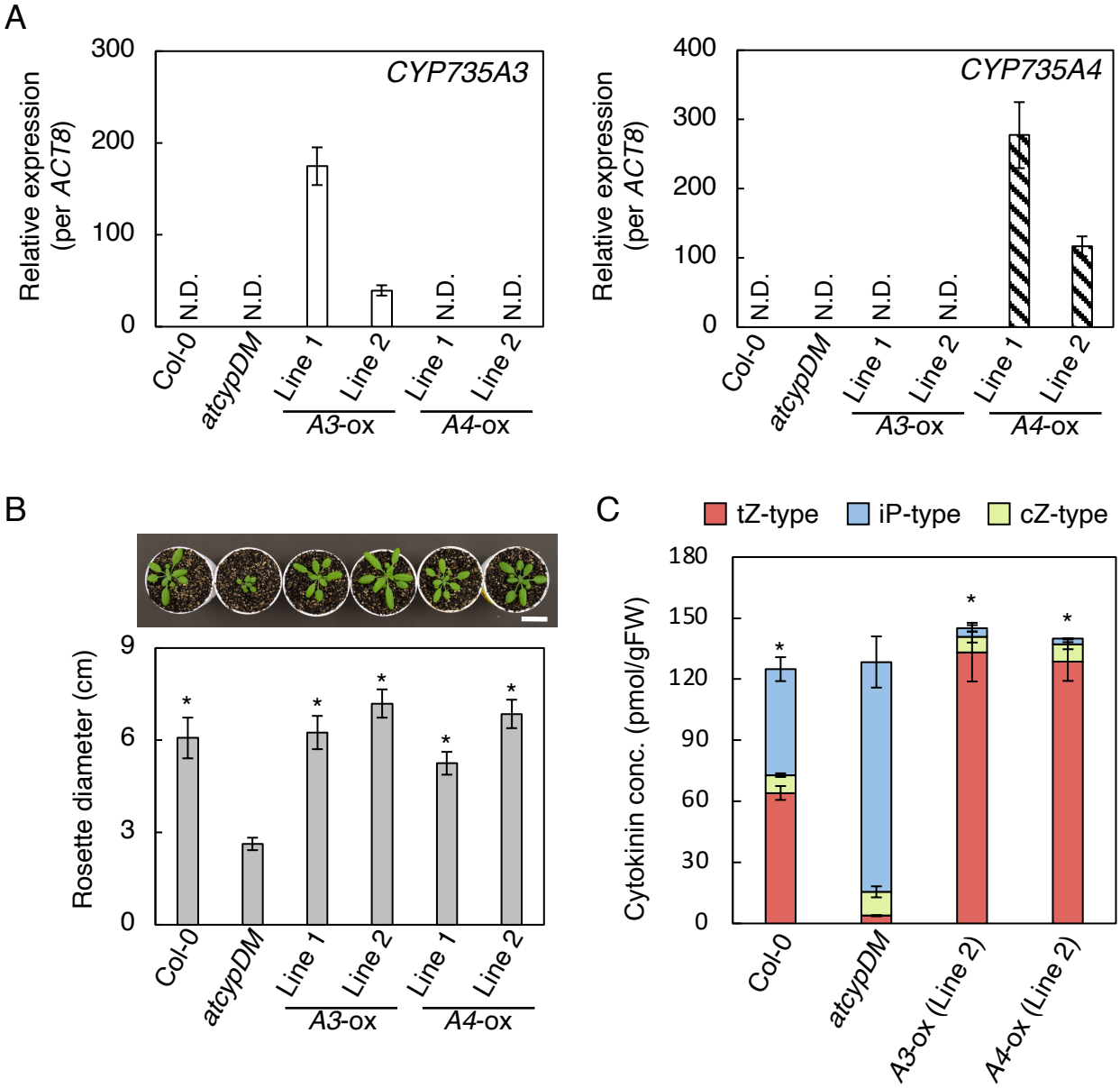

Figure 1. Recovery of *trans*-zeatin-type cytokinin deficiency in the *Arabidopsis* mutant *cyp735a1 cyp735a2* by *CYP735A3* or *CYP735A4*

(A) Quantitative RT-PCR analysis of *CYP735A3* (left) or *CYP735A4* (right) expression in whole seedlings of Col-0, *cyp735a1 cyp735a2* mutant (*atcypDM*), and transgenic plants constitutively expressing *CYP735A3* (*A3*-ox) or *CYP735A4* (*A4*-ox) in *atcypDM* background. Seedlings were grown on 1/2x MS agar plates for 12 days before harvest. Expression levels were normalized using *ACT8* as an internal control. Error bars represent standard deviation (n=4 independent pools of more than ten plants). N.D., under the quantification detection limit. (B) Rosette diameter of 28-day-old Col-0, *atcypDM,* and transgenic plants constitutively expressing *CYP735A3* (*A3*-ox) or *CYP735A4* (*A4*-ox) in *atcypDM* background grown on soil. A photograph of representative plants is shown. Error bars represent standard deviation (n=7). Asterisks indicate statistically significant differences compared with *atcypDM* ($p<0.01$, Student's *t*-test). Scale bar, 3 cm. (C) Cytokinin concentrations in whole seedlings of Col-0, *atcypDM* and transgenic plants constitutively expressing *CYP735A3* (*A3*-ox) or *CYP735A4* (*A4*-ox) in *atcypDM* background. Seedlings were grown on 1/2x MS agar plates for 12 days before harvest. Error bars represent standard deviation (n=4 independent pools of more than ten plants). Asterisks indicate statistically significant differences in tZ-type cytokinin concentration compared with *atcypDM* ($p<0.01$, Student's *t*-test). The concentration of each cytokinin molecular species in roots and shoots is shown in Table S1. gFW, gram fresh weight; tZ-type, *trans*-zeatin and its conjugates; cZ-type, *cis*-zeatin and its conjugates; iP-type, N^6-(Δ^2-isopentenyl)adenine and its conjugates.

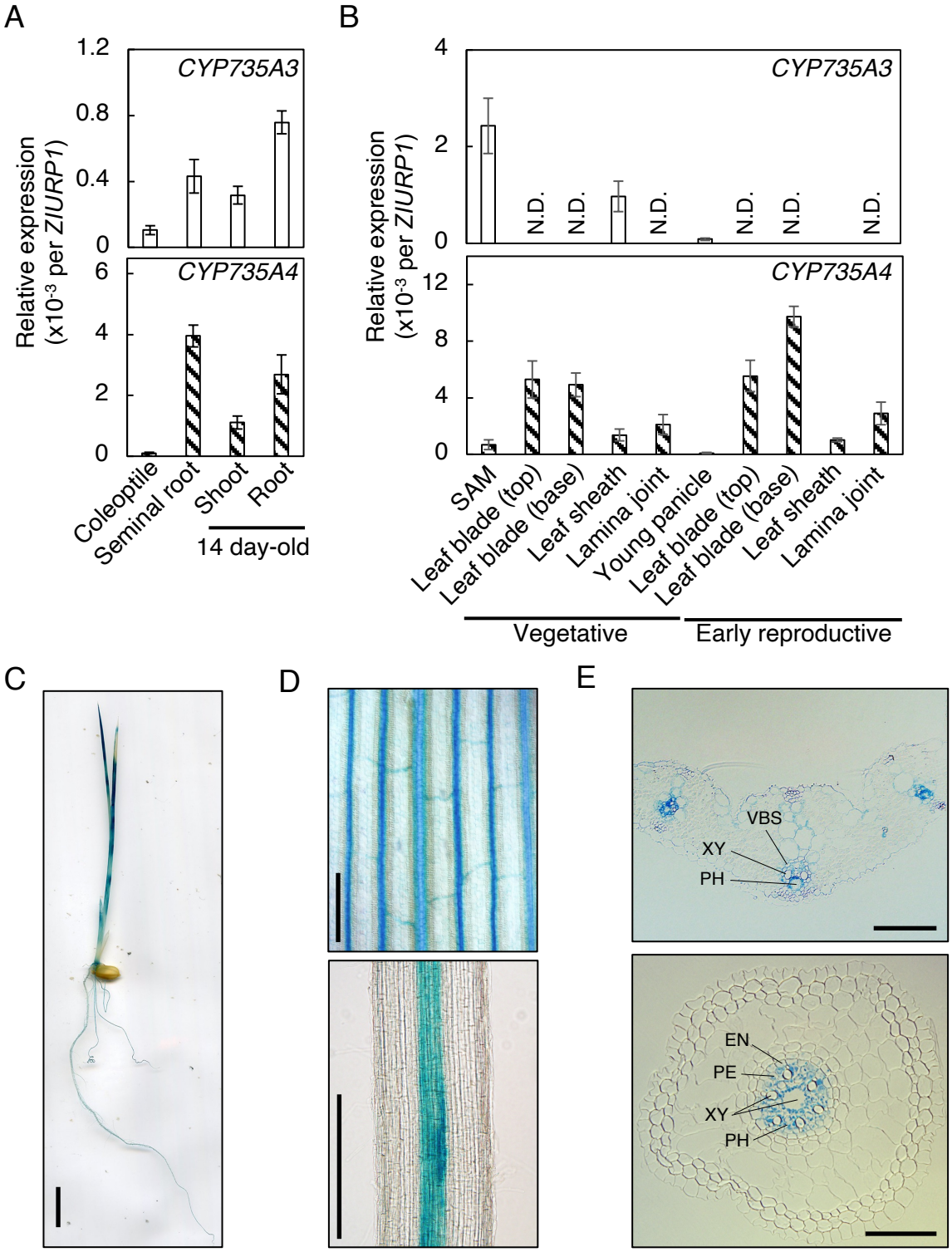

Figure 2. Expression pattern of *CYP735A3* and *CYP735A4* in various tissues

(A) Expression of *CYP735A3* and *CYP735A4* in Nipponbare seedlings. Coleoptiles and seminal roots, and roots and shoots were harvested 4 days and 14 days, respectively, after imbibition. Error bars represent standard deviation of biological replicates (n=4-5 independent pools of more than 2 plants). (B) Expression of *CYP735A3* and *CYP735A4* in Nipponbare plants in vegetative or early reproductive stages. 42-day-old (vegetative stage) and older plants (reproductive stage) were used. The shoot apex parts of 42-day-old plants were collected as shoot apical meristem (SAM). Leaf blade, leaf sheath and lamina joint were harvested from the youngest fully expanded leaf. The young panicle is a mixture of 2 mm to 21 mm long young panicles collected from plants at the reproductive stage. Error bars represent standard deviation of biological replicates (n=4 except for SAM and young panicle, n=4 and n=7 independent pools of more than 2 plants for SAM and young panicle, respectively). N.D., under the quantification detection limit. (C-E) Representative images of GUS staining obtained from *proCYP735A3:GUS* transgenic seedlings grown for 8 days after imbibition. Pictures of a whole seedling (C), first leaf (D, upper), crown root (D, lower), cross section of the first leaf (E, upper), and cross section of seminal root (E, lower) are presented. VBS, vascular bundle sheath; XY, xylem; PH, phloem; EN, endodermis; PE, pericycle. Scale bars, (C) 1 cm; (D) 200 μm; (E) 50 μm.

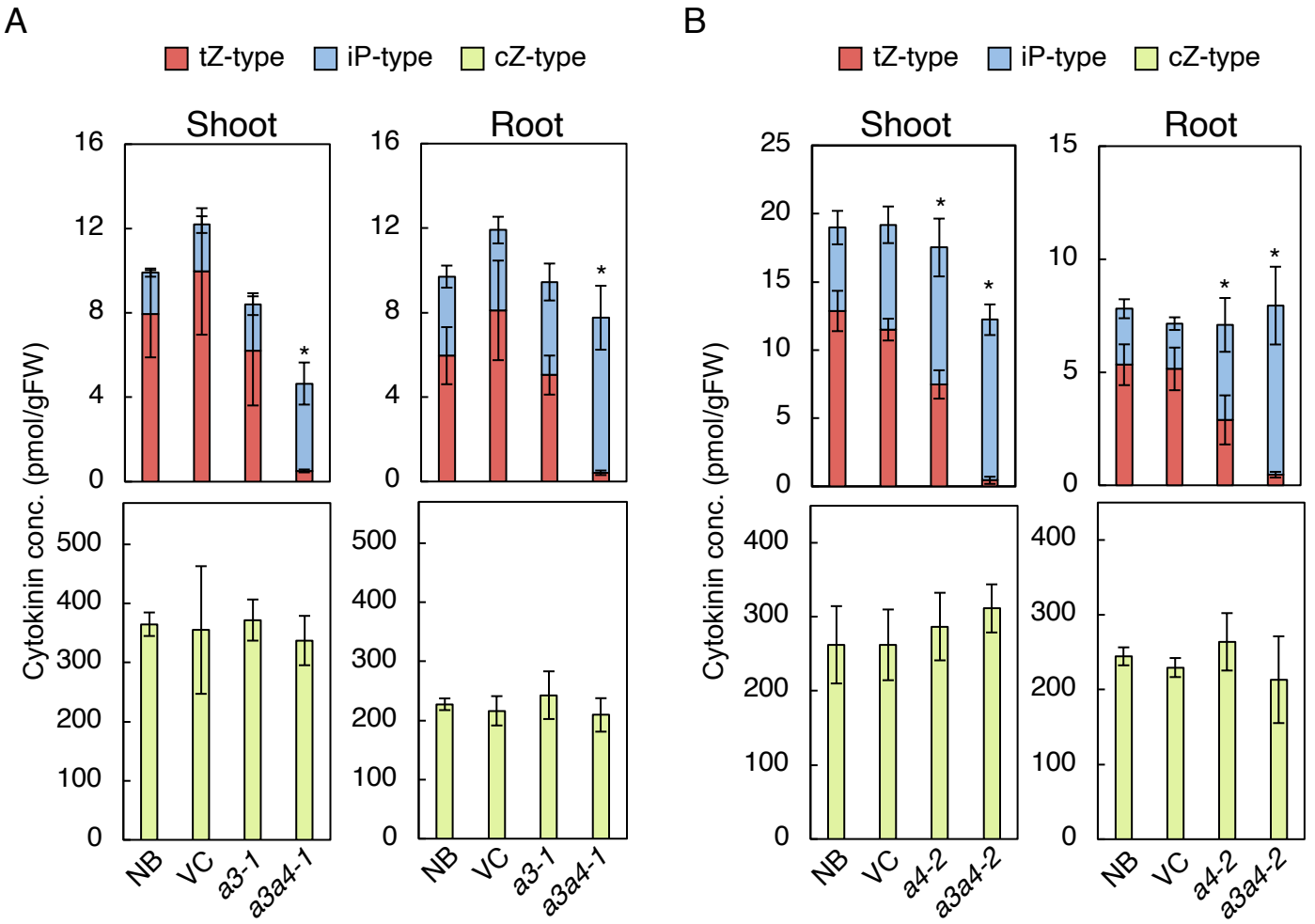

Figure 3. The *cyp735a3 cyp735a4* double mutants show deficiency in *trans*-zeatin-type cytokinins
Cytokinin concentrations in roots and shoots of WT strain Nipponbare (NB), vector control (VC), and mutant strains *cyp735a3-1* (*a3-1*), *cyp735a4-2* (*a4-2*), *cyp735a3-1 cyp735a4-1* (*a3a4-1*), and *cyp735a3-2 cyp735a4-2* (*a3a4-2*). Seedlings were grown hydroponically for 14 days (A) or 12 days (B) before shoots and roots were harvested. Error bars represent standard deviation of biological replicates (n=3-6 independent pools of more than ten plants for A, n=6-8 independent pools of more than ten plants for B). Asterisks indicate statistically significant differences in tZ-type cytokinin concentration compared with NB ($p<0.05$, Student's *t*-test). The concentration of each cytokinin molecular species in roots and shoots is shown in Table S2 and Table S3. gFW, gram fresh weight; tZ-type, *trans*-zeatin and its conjugates; cZ-type, *cis*-zeatin and its conjugates; iP-type, N^6-(Δ^2-isopentenyl)adenine and its conjugates.

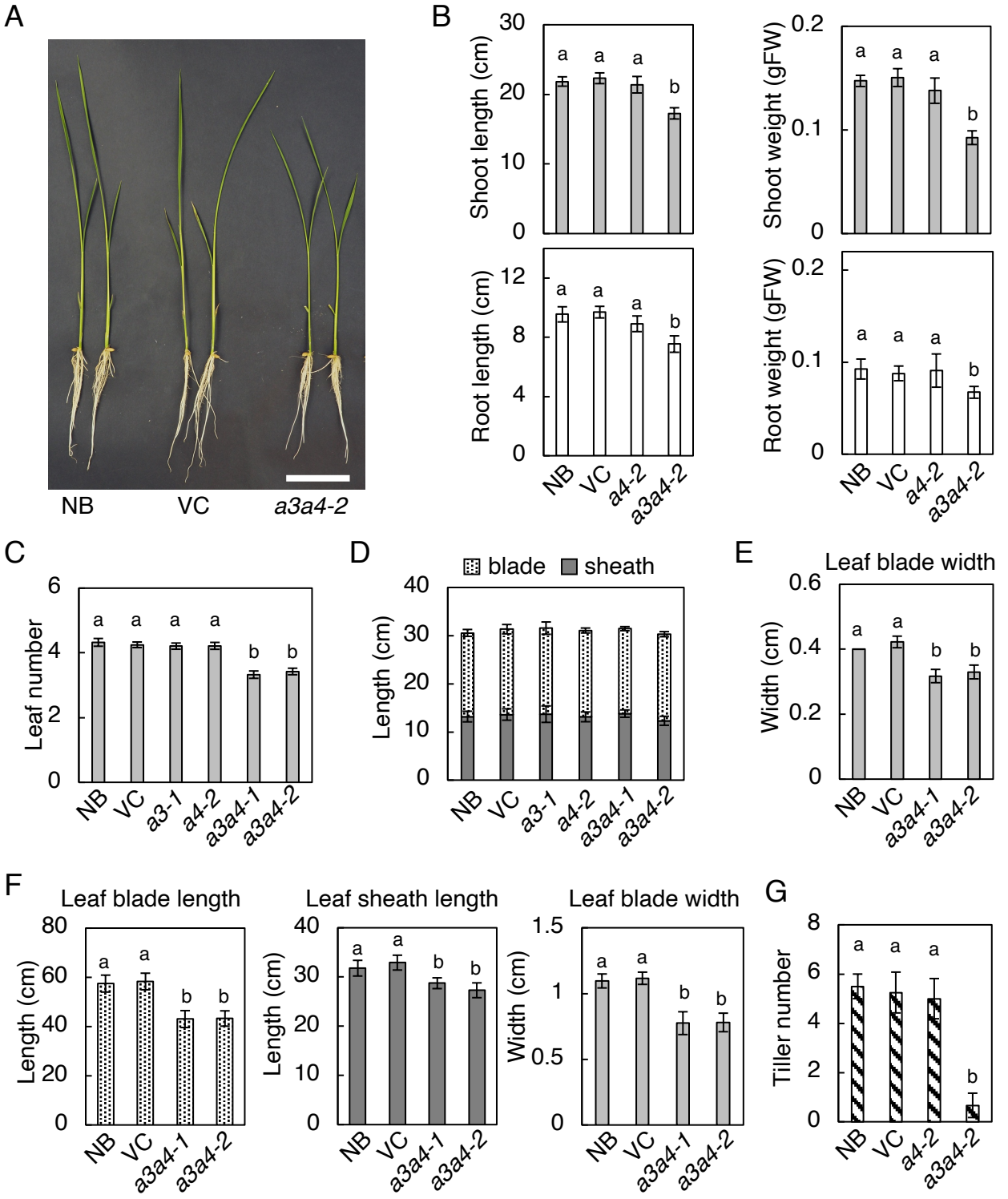

Figure 4. Disruption of *CYP735A*s alters rice growth in seedling to vegetative phases
(A) A representative image of Nipponbare (NB), vector control (VC), and *cyp735a3-2 cyp735a4-2* (*a3a4-2*) seedlings grown 12 days in hydroponic culture. Scale bar, 5 cm. (B) Quantification of shoot length, shoot fresh weight, root length, and root fresh weight in 12-day-old seedlings. NB, VC, *cyp735a4-2* (*a4-2*), and *a3a4-2* seedlings were grown in hydroponic culture. (C) Leaf number at 15 days after germination (D, E) Leaf sheath and leaf blade length (D) and leaf width (E) of the fully expanded third leaf of NB, VC, *cyp735a3-1* (*a3-1*), *cyp735a4-2* (*a4-2*), *cyp735a3-1 cyp735a4-1* (*a3a4-1*), and *a3a4-2* seedlings grown on soil. (F) Quantification of leaf blade length, leaf sheath length, and leaf width of the fully expanded ninth leaf in NB, VC, *a3a4-1*, and *a3a4-2* grown on soil. (G) Tiller number of NB, VC, *a3a4-1*, and *a3a4-2* grown on soil for 35 days. Error bars represent standard deviation of biological replicates (B, n=6-8; C, n=8-12; D, n=8-10; E, n=8-10; F, n=8-12; G, n=4-8). Different lowercase letters indicate statistically significant differences as indicated by Tukey's HSD test ($p<0.05$).

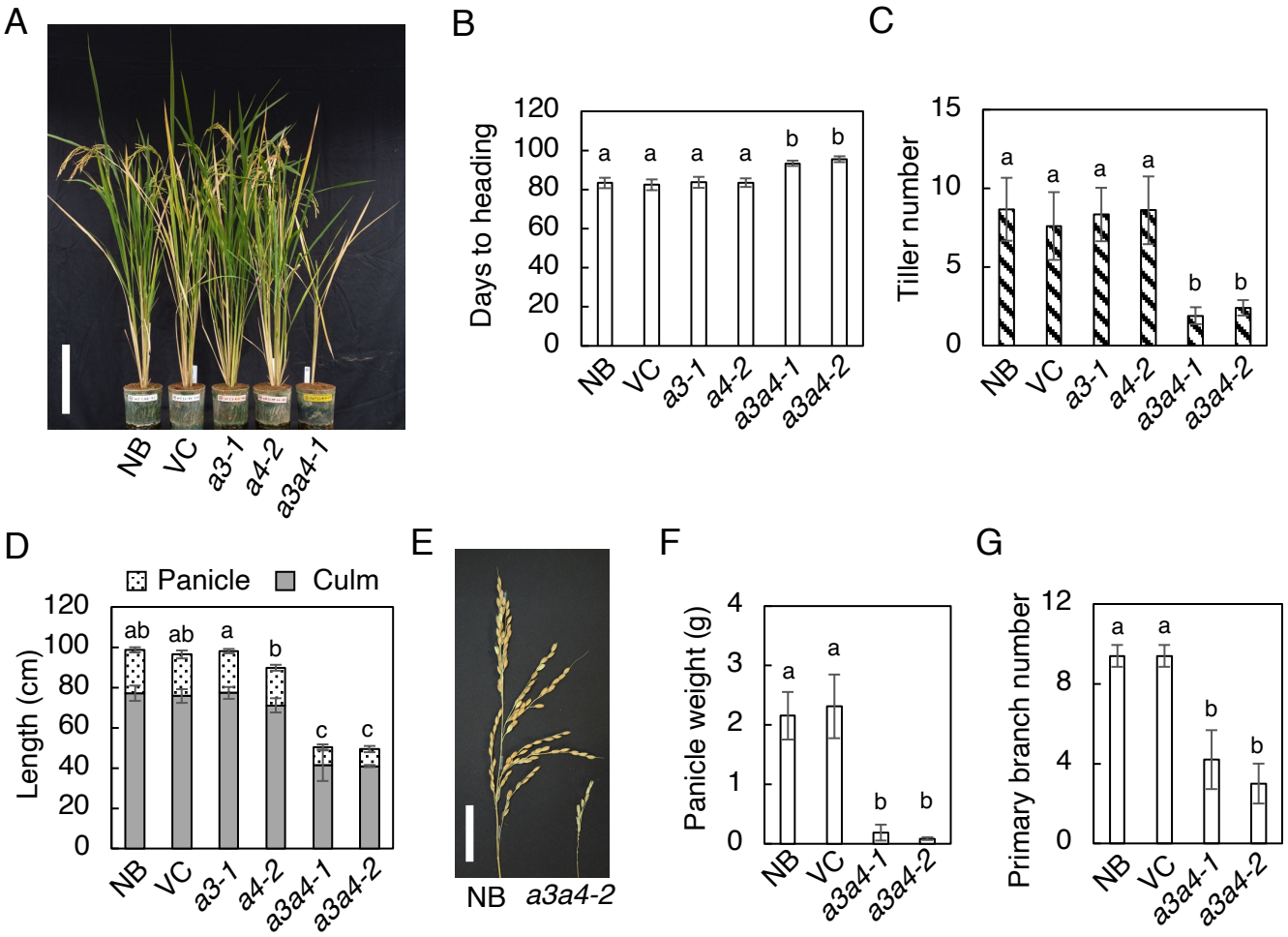

Figure 5. Disruption of *CYP735A*s alters rice growth in reproductive to maturatation phases
(A) A representative image of Nipponbare (NB), vector control (VC), and *cyp735a3-1* (*a3-1*), *cyp735a4-1* (*a4-2*), and *cyp735a3-1 cyp735a4-1* (*a3a4-2*) plants grown 15 weeks on soil. Scale bar, 20 cm. (B-D) Heading date (B), panicle and culm length (C), and tiller number (D) of NB, VC, *a3-1*, *a4-2*, *cyp735a3-1 cyp735a4-1* (*a3a4-1*), and *a3a4-2*. (E) A representative picture of mature panicles from NB and *a3a4-2*. Scale bar, 5 cm. (F, G) Panicle weight on the main stem (F) and number of primary branches per panicle (G). Error bars represent standard deviation of biological replicates (B, n=3-12; C, n=5-12; D, n=9-12; F, n=5-10; G, n=5-10). Different lowercase letters indicate statistically significant differences as indicated by Tukey's HSD test ($p<0.05$).

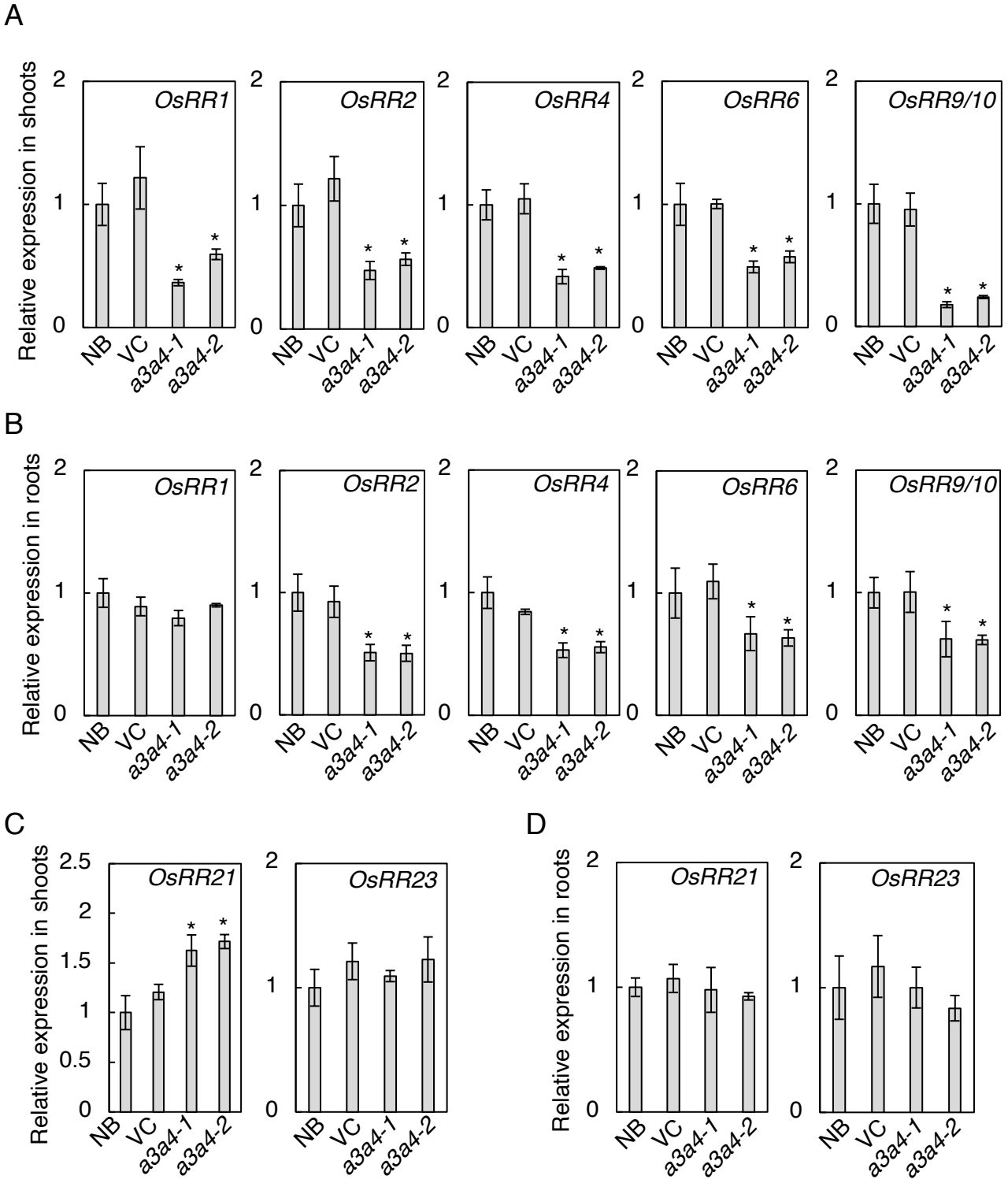

Figure 6. Expression of cytokinin inducible type-A response regulator genes is altered in the *cyp735a3 cyp735a4* mutant

(A, B) Transcript levels of cytokinin inducible type-A response regulator genes, *OsRR1*, *OsRR2*, *OsRR*4, *OsRR6*, and *OsRR9/10*, in shoots (A) and roots (B) of Nipponbare (NB), vector control (VC), *cyp735a3-1 cyp735a4-1* (*a3a4-1*) and *cyp735a3-2 cyp735a4-2* (*a3a4-2*) seedlings. *OsRR9/10* indicates that the primer set used could not distinguish *OsRR9* and *OsRR10*. (C, D) Transcript levels of type-B response regulator genes, *OsRR21* and *OsRR23*, in the shoot. (C) and in the root (D) of NB, VC, *a3a4-1* and *a3a4-2* seedlings. Seedlings were grown hydroponically for 10 days before roots and shoots were harvested. Expression levels were quantified by qRT-PCR analysis, normalized to *ZIURP1* as an internal control, and are shown relative to the value of NB. Error bars represent standard deviation of biological replicates (n=4 independent pools of 2 plants). Asterisks indicate statistically significant differences compared to NB ($p<0.05$, Student's *t*-test).

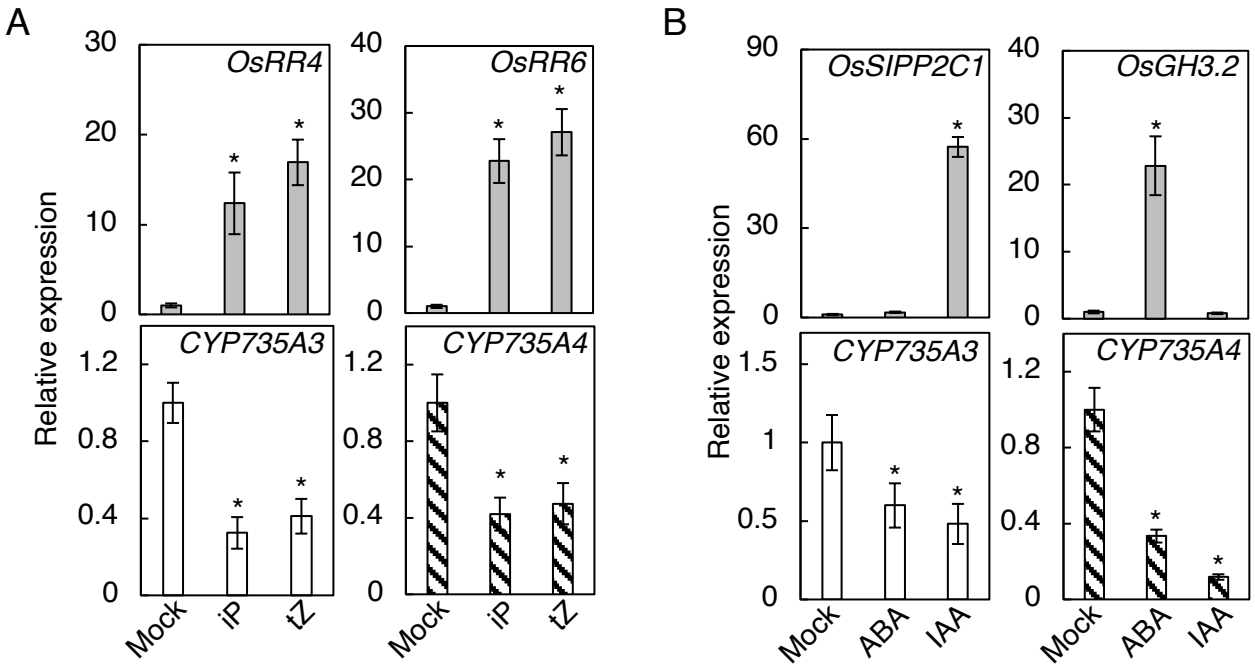

Figure 7. Expression of *CYP735A3* and *CYP735A4* in response to phytohormones
(A) Expression of *CYP735A*s in response to cytokinin. Nipponbare (NB) seedlings grown for 12 days were treated with 0.001% DMSO (Mock), 1 μM iP (iP), or 1 μM tZ (tZ) and roots were harvested after 2 h. (B) Expression of *CYP735A*s in response to abscisic acid (ABA) and auxin. NB seedlings grown for 12 days were treated with 0.05% DMSO (Mock), 10 μM indole-3-acetic acid (IAA) or 50 μM ABA and roots were harvested after 2 h. Expression levels were quantified by qRT-PCR analysis, normalized to *ZIURP1* as an internal control, and are shown relative to the value in mock treatment. Asterisks indicate statistically significant differences compared with Mock ($p<0.05$, Student's *t*-test). Error bars represent standard deviation (n=4 independent pools of more than 2 plants).

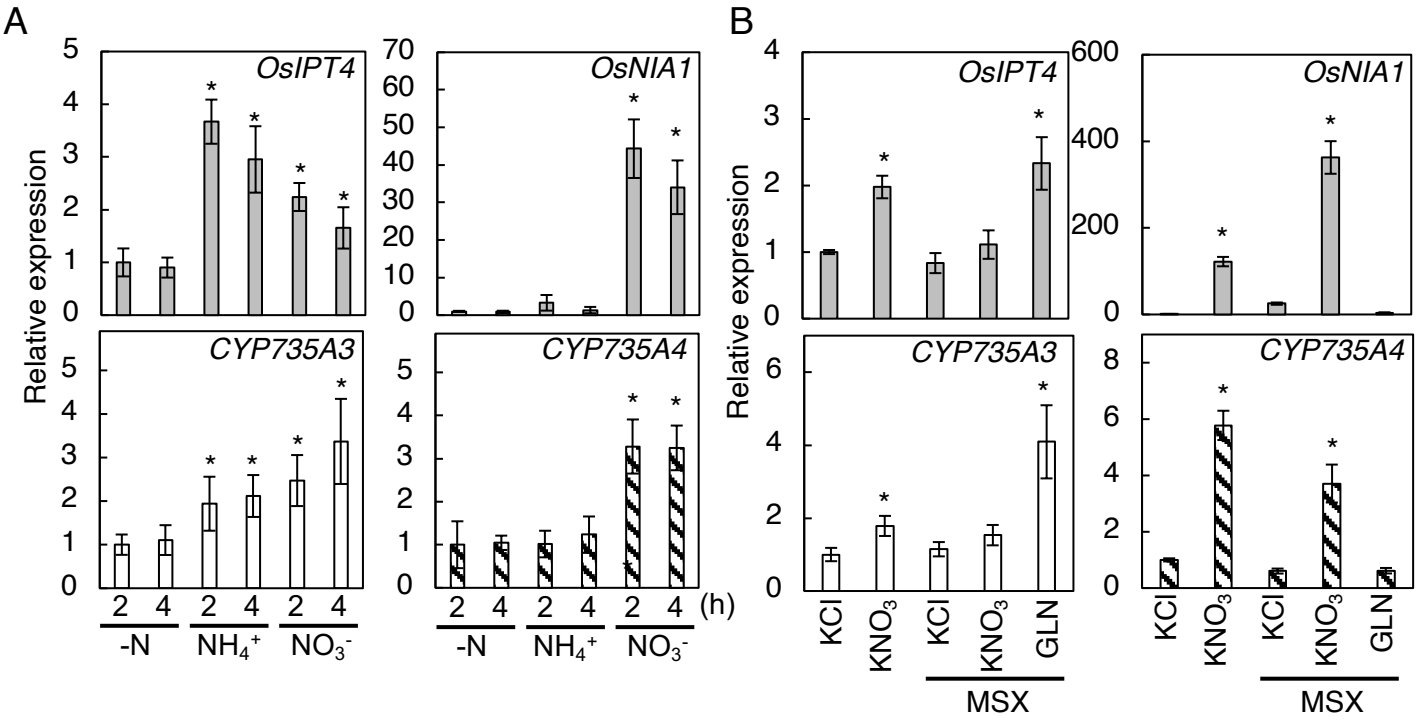

Figure 8. Expression of *CYP735A3* and *CYP735A4* in response to nitrogen sources in roots
(A) Expression of *CYP735A*s in response to ammonium or nitrate supplement. Twelve day-old NB seedlings hydroponically grown in nitrogen-free nutrient solution were incubated with 5 mM KCl (-N), 5 mM NH_4Cl (NH_4^+), or 5 mM KNO_3 (NO_3^-) for 2 h or 4 h. Expression levels were quantified by qRT-PCR analysis, normalized to *ZIURP1* as an internal control, and are shown relative to the value in 2 h of -N treatment. Error bars represent standard deviation (n=4 independent pools of 3 plants). (B) Effect of methionine sulfoximine on the induction of *CYP735A*s by nitrogen. Twelve day-old NB seedlings hydroponically grown in nitrogen-free nutrient solution were pre-treated with 2 mM MSX for 2 h and then incubated with 5 mM KCl, 5 mM KNO_3 or 50 mM glutamine (GLN) for 2 h. Asterisks indicate statistically significant differences compared with KCl or KCl+MSX (($p<0.05$, Student's *t*-test)). Expression levels were quantified by qRT-PCR analysis, normalized to *ZIURP1* as an internal control, and are shown relative to the value in KCl treatment. Error bars represent standard deviation (n=4 independent pools of 3 plants).

Parsed Citations

Bassil N V, Mok D, Mok MC (1993) Partial purification of a cis-trans-isomerase of zeatin from immature seed of Phaseolus vulgaris L. Plant Physiol 102: 867–872
Google Scholar: Author Only Title Only Author and Title

Burr CA, Sun J, Yamburenko M V., Willoughby A, Hodgens C, Boeshore SL, Elmore A, Atkinson J, Nimchuk ZL, Bishopp A, et al (2021) The HK5 and HK6 cytokinin receptors mediate diverse developmental pathways in rice. Development 147: dev191734
Google Scholar: Author Only Title Only Author and Title

Cai L, Zhang L, Fu Q, Xu ZF (2018) Identification and expression analysis of cytokinin metabolic genes IPTs, CYP735A and CKXs in the biofuel plant Jatropha curcas. PeerJ 2018: e4812
Google Scholar: Author Only Title Only Author and Title

Chanch T, Ohira K (1982) Comparison of the uptake and assimilation of ammonium and nitrate in indica and japonica rice plants using the tracer 15N method. Soil Sci Plant Nutr 28: 79–90
Google Scholar: Author Only Title Only Author and Title

Choi J, Lee J, Kim K, Cho M, Ryu H, An G, Hwang I (2012) Functional identification of OsHk6 as a homotypic cytokinin receptor in rice with preferential affinity for iP. Plant Cell Physiol 53: 1334–1343
Google Scholar: Author Only Title Only Author and Title

Clough SJ, Bent AF (1998) Floral dip: a simplified method for Agrobacterium-mediated transformation of Arabidopsis thaliana. Plant J 16: 735–743
Google Scholar: Author Only Title Only Author and Title

Coskun D, Britto DT, Shi W, Kronzucker HJ (2017) Nitrogen transformations in modern agriculture and the role of biological nitrification inhibition. Nat Plants 3: 17074
Google Scholar: Author Only Title Only Author and Title

Du H, Wu N, Fu J, Wang S, Li X, Xiao J, Xiong L (2012) A GH3 family member, OsGH3-2, modulates auxin and abscisic acid levels and differentially affects drought and cold tolerance in rice. J Exp Bot 63: 6467–6480
Google Scholar: Author Only Title Only Author and Title

Engelsberger WR, Schulze WX (2012) Nitrate and ammonium lead to distinct global dynamic phosphorylation patterns when resupplied to nitrogen-starved Arabidopsis seedlings. Plant J 69: 978–995
Google Scholar: Author Only Title Only Author and Title

Gajdošová S, Spíchal L, Kamínek M, Hoyerová K, Novák O, Dobrev PI, Galuszka P, Klíma P, Gaudinová A, Žižková E, et al (2011) Distribution, biological activities, metabolism, and the conceivable function of cis-zeatin-type cytokinins in plants. J Exp Bot 62: 2827–2840
Google Scholar: Author Only Title Only Author and Title

Hansen CC, Nelson DR, Møller BL, Werck-Reichhart D (2021) Plant cytochrome P450 plasticity and evolution. Mol Plant 14: 1244–1265
Google Scholar: Author Only Title Only Author and Title

Hirose N, Makita N, Kojima M, Kamada-Nobusada T, Sakakibara H (2007) Overexpression of a type-A response regulator alters rice morphology and cytokinin metabolism. Plant Cell Physiol 48: 523–539
Google Scholar: Author Only Title Only Author and Title

Hirose N, Makita N, Yamaya T, Sakakibara H (2005) Functional characterization and expression analysis of a gene, OsENT2, encoding an equilibrative nucleoside transporter in rice suggest a function in cytokinin transport. Plant Physiol 138: 196–206
Google Scholar: Author Only Title Only Author and Title

Hirose N, Takei K, Kuroha T, Kamada-Nobusada T, Hayashi H, Sakakibara H (2008) Regulation of cytokinin biosynthesis, compartmentalization and translocation. J Exp Bot 59: 75–83
Google Scholar: Author Only Title Only Author and Title

Kakimoto T (2001) Identification of plant cytokinin biosynthetic enzymes as dimethylallyl diphosphate : ATP/ADP isopentenyltransferases. Plant Cell Physiol 42: 677–685
Google Scholar: Author Only Title Only Author and Title

Kamada-Nobusada T, Makita N, Kojima M, Sakakibara H (2013) Nitrogen-dependent regulation of de novo cytokinin biosynthesis in rice: the role of glutamine metabolism as an additional signal. Plant Cell Physiol 54: 1881–1893
Google Scholar: Author Only Title Only Author and Title

Kawai M, Tabata R, Ohashi M, Honda H, Kamiya T, Kojima M, Takebayashi Y, Oishi S, Okamoto S, Hachiya T, et al (2022) Regulation of ammonium acquisition and use in Oryza longistaminata ramets under nitrogen source heterogeneity. Plant Physiol 188: 2364–2376

Google Scholar: Author Only Title Only Author and Title

Kiba T, Inaba J, Kudo T, Ueda N, Konishi M, Mitsuda N, Takiguchi Y, Kondou Y, Yoshizumi T, Ohme-Takagi M, et al (2018) Repression of nitrogen-starvation responses by members of the Arabidopsis GARP-type transcription factor NIGT1/HRS1 subfamily. Plant Cell 30: 925–945
Google Scholar: Author Only Title Only Author and Title

Kiba T, Kudo T, Kojima M, Sakakibara H (2011) Hormonal control of nitrogen acquisition: roles of auxin, abscisic acid, and cytokinin. J Exp Bot 62: 1399–1409
Google Scholar: Author Only Title Only Author and Title

Kiba T, Takebayashi Y, Kojima M, Sakakibara H (2019) Sugar-induced de novo cytokinin biosynthesis contributes to Arabidopsis growth under elevated CO2. Sci Rep 9: 1–15
Google Scholar: Author Only Title Only Author and Title

Kiba T, Takei K, Kojima M, Sakakibara H (2013) Side-chain modification of cytokinins controls shoot growth in Arabidopsis. Dev Cell 27: 452–461
Google Scholar: Author Only Title Only Author and Title

Kieber JJ, Schaller GE (2018) Cytokinin signaling in plant development. Development 145: dev149344
Google Scholar: Author Only Title Only Author and Title

Kirk GJ, Kronzucker HJ (2005) The potential for nitrification and nitrate uptake in the rhizosphere of wetland plants: a modelling study. Ann Bot 96: 639–646
Google Scholar: Author Only Title Only Author and Title

Kojima M, Kamada-Nobusada T, Komatsu H, Takei K, Kuroha T, Mizutani M, Ashikari M, Ueguchi-Tanaka M, Matsuoka M, Suzuki K, et al (2009) Highly sensitive and high-throughput analysis of plant hormones using MS-probe modification and liquid chromatography tandem mass spectrometry: an application for hormone profiling in Oryza sativa. Plant Cell Physiol 50: 1201–1214
Google Scholar: Author Only Title Only Author and Title

Kojima M, Sakakibara H (2012) Highly sensitive high-throughput profiling of six phytohormones using MS-probe modification and liquid chromatography-tandem mass spectrometry. Methods Mol Biol 918: 151–164
Google Scholar: Author Only Title Only Author and Title

Kudo T, Makita N, Kojima M, Tokunaga H, Sakakibara H (2012) Cytokinin activity of cis-zeatin and phenotypic alterations induced by overexpression of putative cis-Zeatin-O-glucosyltransferase in rice. Plant Physiol 160: 319–331
Google Scholar: Author Only Title Only Author and Title

Kurakawa T, Ueda N, Maekawa M, Kobayashi K, Kojima M, Nagato Y, Sakakibara H, Kyozuka J (2007) Direct control of shoot meristem activity by a cytokinin-activating enzyme. Nature 445: 652–655
Google Scholar: Author Only Title Only Author and Title

Kuroha T, Tokunaga H, Kojima M, Ueda N, Ishida T, Nagawa S, Fukuda H, Sugimoto K, Sakakibara H (2009) Functional analyses of LONELY GUY cytokinin-activating enzymes reveal the importance of the direct activation pathway in Arabidopsis. Plant Cell 21: 3152–3169
Google Scholar: Author Only Title Only Author and Title

Labun K, Montague TG, Krause M, Torres Cleuren YN, Tjeldnes H, Valen E (2019) CHOPCHOP v3: Expanding the CRISPR web toolbox beyond genome editing. Nucleic Acids Res 47: W171–W174
Google Scholar: Author Only Title Only Author and Title

Lam HM, Coschigano KT, Oliveira IC, Melo-Oliveira R, Coruzzi GM (1996) The molecular-genetics of nitrogen assimilation into amino acids in higher plants. Annu Rev Plant Physiol Plant Mol Biol 47: 569–593
Google Scholar: Author Only Title Only Author and Title

Li YS, Sun H, Wang ZF, Duan M, Huang SD, Yang J, Huang J, Zhang HS (2013) A novel nuclear protein phosphatase 2C negatively regulated by ABL1 is involved in abiotic stress and panicle development in rice. Mol Biotechnol 54: 703–710
Google Scholar: Author Only Title Only Author and Title

Lomin SN, Yonekura-Sakakibara K, Romanov GA, Sakakibara H (2011) Ligand-binding properties and subcellular localization of maize cytokinin receptors. J Exp Bot 62: 5149–5159
Google Scholar: Author Only Title Only Author and Title

Macková H, Hronková M, Dobrá J, Turečková V, Novák O, Lubovská Z, Motyka V, Haisel D, Hájek T, Prášil IT, et al (2013) Enhanced drought and heat stress tolerance of tobacco plants with ectopically enhanced cytokinin oxidase/dehydrogenase gene expression. J Exp Bot 64: 2805–2815
Google Scholar: Author Only Title Only Author and Title

Maeda Y, Konishi M, Kiba T, Sakuraba Y, Sawaki N, Kurai T, Ueda Y, Sakakibara H, Yanagisawa S (2018) A NIGT1-centred transcriptional cascade regulates nitrate signalling and incorporates phosphorus starvation signals in Arabidopsis. Nat Commun

9: 1–14
Google Scholar: Author Only Title Only Author and Title

Makino A, Mae T, Ohira K (1985) Photosynthesis and ribulose-1,5-bisphosphate carboxylase oxygenase in rice leaves from emergence through senescence - quantitative-analysis by carboxylation oxygenation and regeneration of ribulose 1,5-bisphosphate. Planta 166: 414–420
Google Scholar: Author Only Title Only Author and Title

Midlik A, Navrátilová V, Moturu TR, Koča J, Svobodová R, Berka K (2021) Uncovering of cytochrome P450 anatomy by SecStrAnnotator. Sci Rep 11: 12345
Google Scholar: Author Only Title Only Author and Title

Miyawaki K, Matsumoto-Kitano M, Kakimoto T (2004) Expression of cytokinin biosynthetic isopentenyltransferase genes in Arabidopsis: tissue specificity and regulation by auxin, cytokinin, and nitrate. Plant J 37: 128–138
Google Scholar: Author Only Title Only Author and Title

Miyawaki K, Tarkowski P, Matsumoto-Kitano M, Kato T, Sato S, Tarkowska D, Tabata S, Sandberg G, Kakimoto T (2006) Roles of Arabidopsis ATP/ADP isopentenyltransferases and tRNA isopentenyltransferases in cytokinin biosynthesis. Proc Natl Acad Sci USA 103: 16598–16603
Google Scholar: Author Only Title Only Author and Title

Mok DW, Mok MC (2001) Cytokinin metabolism and action. Annu Rev Plant Physiol Plant Mol Biol 52: 89–118
Google Scholar: Author Only Title Only Author and Title

Mok MC, Mok DW, Armstrong DJ (1978) Differential cytokinin structure-activity relationships in Phaseolus. Plant Physiol 61: 72–75
Google Scholar: Author Only Title Only Author and Title

Nacry P, Bouguyon E, Gojon A (2013) Nitrogen acquisition by roots: physiological and developmental mechanisms ensuring plant adaptation to a fluctuating resource. Plant Soil 370: 1–29
Google Scholar: Author Only Title Only Author and Title

Ohashi M, Ishiyama K, Kojima S, Kojima M, Sakakibara H, Yamaya T, Hayakawa T (2017) Lack of cytosolic glutamine synthetase1;2 activity reduces nitrogen-dependent biosynthesis of cytokinin required for axillary bud outgrowth in rice seedlings. Plant Cell Physiol 58: 679–690
Google Scholar: Author Only Title Only Author and Title

Osugi A, Kojima M, Takebayashi Y, Ueda N, Kiba T, Sakakibara H (2017) Systemic transport of trans-zeatin and its precursor have differing roles in Arabidopsis shoots. Nat Plants 3: 1–6
Google Scholar: Author Only Title Only Author and Title

Osugi A, Sakakibara H (2015) Q&A: How do plants respond to cytokinins and what is their importance? BMC Biol 13: 102

Pabuayon IM, Yamamoto N, Trinidad JL, Longkumer T, Raorane ML, Kohli A (2016) Reference genes for accurate gene expression analyses across different tissues, developmental stages and genotypes in rice for drought tolerance. Rice 9: 32
Google Scholar: Author Only Title Only Author and Title

Romanov GA, Lomin SN, Schmülling T (2006) Biochemical characteristics and ligand-binding properties of Arabidopsis cytokinin receptor AHK3 compared to CRE1/AHK4 as revealed by a direct binding assay. J Exp Bot 57: 4051–4058
Google Scholar: Author Only Title Only Author and Title

Sakakibara H (2006) Cytokinins: activity, biosynthesis, and translocation. Annu Rev Plant Biol 57: 431–449
Google Scholar: Author Only Title Only Author and Title

Sakakibara H (2021) Cytokinin biosynthesis and transport for systemic nitrogen signaling. Plant J 105: 421–430
Google Scholar: Author Only Title Only Author and Title

Schäfer M, Brütting C, Meza-Canales ID, Großkinsky DK, Vankova R, Baldwin IT, Meldau S (2015) The role of cis-zeatin-type cytokinins in plant growth regulation and mediating responses to environmental interactions. J Exp Bot. Oxford University Press, pp 4873–4884
Google Scholar: Author Only Title Only Author and Title

Schmitz RY, Skoog F (1972) Cytokinins: Synthesis and biological activity of geometric and position isomers of zeatin. Plant Physiol 50: 702–705
Google Scholar: Author Only Title Only Author and Title

Shaw G (1994) Chemistry of adenine cytokinins. In DWS Mok, MC Mok, eds, Cytokinins: Chemistry, Activity, and Function. CRC Press, Boca Rato, FL, pp 15–34
Google Scholar: Author Only Title Only Author and Title

Shibasaki K, Takebayashi A, Makita N, Kojima M, Takebayashi Y, Kawai M, Hachiya T, Sakakibara H (2021) Nitrogen nutrition promotes rhizome bud outgrowth via regulation of cytokinin biosynthesis genes and an Oryza longistaminata ortholog of FINE

CULM 1. Front Plant Sci 12: 788
Google Scholar: Author Only Title Only Author and Title

Spíchal L, Rakova NY, Riefler M, Mizuno T, Romanov GA, Strnad M, Schmülling T (2004) Two cytokinin receptors of Arabidopsis thaliana, CRE1/AHK4 and AHK3, differ in their ligand specificity in a bacterial assay. Plant Cell Physiol 45: 1299–1305
Google Scholar: Author Only Title Only Author and Title

Stolz A, Riefler M, Lomin SN, Achazi K, Romanov GA, Schmülling T (2011) The specificity of cytokinin signalling in Arabidopsis thaliana is mediated by differing ligand affinities and expression profiles of the receptors. Plant J 67: 157–168
Google Scholar: Author Only Title Only Author and Title

Takei K, Sakakibara H, Sugiyama T (2001a) Identification of genes encoding adenylate isopentenyltransferase, a cytokinin biosynthesis enzyme, in Arabidopsis thaliana. J Biol Chem 276: 26405–26410
Google Scholar: Author Only Title Only Author and Title

Takei K, Sakakibara H, Taniguchi M, Sugiyama T (2001b) Nitrogen-dependent accumulation of cytokinins in root and the translocation to leaf: implication of cytokinin species that induces gene expression of maize response regulator. Plant Cell Physiol 42: 85–93
Google Scholar: Author Only Title Only Author and Title

Takei K, Yamaya T, Sakakibara H (2004) Arabidopsis CYP735A1 and CYP735A2 encode cytokinin hydroxylases that catalyze the biosynthesis of trans-zeatin. J Biol Chem 279: 41866–41872
Google Scholar: Author Only Title Only Author and Title

Toda E, Koiso N, Takebayashi A, Ichikawa M, Kiba T, Osakabe K, Osakabe Y, Sakakibara H, Kato N, Okamoto T (2019) An efficient DNA- and selectable-marker-free genome-editing system using zygotes in rice. Nat Plants 5: 363–368
Google Scholar: Author Only Title Only Author and Title

Tokunaga H, Kojima M, Kuroha T, Ishida T, Sugimoto K, Kiba T, Sakakibara H (2012) Arabidopsis lonely guy (LOG) multiple mutants reveal a central role of the LOG-dependent pathway in cytokinin activation. Plant J 69: 355–365
Google Scholar: Author Only Title Only Author and Title

Tsai Y-C, Weir NR, Hill K, Zhang W, Kim HJ, Shiu S-H, Schaller GE, Kieber JJ (2012) Characterization of Genes Involved in Cytokinin Signaling and Metabolism from Rice. Plant Physiol 158: 1666–1684
Google Scholar: Author Only Title Only Author and Title

Vanková R, Kosová K, Dobrev P, Vítámvás P, Trávníčková A, Cvikrová M, Pešek B, Gaudinová A, Prerostová S, Musilová J, et al (2014) Dynamics of cold acclimation and complex phytohormone responses in Triticum monococcum lines G3116 and DV92 differing in vernalization and frost tolerance level. Environ Exp Bot 101: 12–25
Google Scholar: Author Only Title Only Author and Title

Vyroubalová S, Václavíková K, Turečková V, Novák O, Šmehilová M, Hluska T, Ohnoutková L, Frébort I, Galuszka P (2009) Characterization of new maize genes putatively involved in cytokinin metabolism and their expression during osmotic stress in relation to cytokinin levels. Plant Physiol 151: 433–447
Google Scholar: Author Only Title Only Author and Title

Werner T, Motyka V, Laucou V, Smets R, Van Onckelen H, Schmülling T (2003) Cytokinin-deficient transgenic Arabidopsis plants show multiple developmental alterations indicating opposite functions of cytokinins in the regulation of shoot and root meristem activity. Plant Cell 15: 2532–2550
Google Scholar: Author Only Title Only Author and Title

Werner T, Schmülling T (2009) Cytokinin action in plant development. Curr Opin Plant Biol 12: 527–538
Google Scholar: Author Only Title Only Author and Title

Worthen JM, Yamburenko M V, Lim J, Nimchuk ZL, Kieber JJ, Schaller GE (2019) Type-B response regulators of rice play key roles in growth, development and cytokinin signaling. Development 146: dev174870
Google Scholar: Author Only Title Only Author and Title

Xu GH, Fan XR, Miller AJ (2012) Plant nitrogen assimilation and use efficiency. Annu Rev Plant Biol 63: 153–182
Google Scholar: Author Only Title Only Author and Title

Yan M, Fan XR, Feng HM, Miller AJ, Shen QR, Xu GH (2011) Rice OsNAR2.1 interacts with OsNRT2.1, OsNRT2.2 and OsNRT2.3a nitrate transporters to provide uptake over high and low concentration ranges. Plant Cell Environ 34: 1360–1372
Google Scholar: Author Only Title Only Author and Title

Yonekura-Sakakibara K, Kojima M, Yamaya T, Sakakibara H (2004) Molecular characterization of cytokinin-responsive histidine kinases in maize. differential ligand preferences and ¥response to cis-zeatin. Plant Physiol 134: 1654–1661
Google Scholar: Author Only Title Only Author and Title

Zhao J, Yu N, Ju M, Fan B, Zhang Y, Zhu E, Zhang M, Zhang K (2019) ABC transporter OsABCG18 controls the shootward

transport of cytokinins and grain yield in rice. J Exp Bot 70: 6277–6291
Google Scholar: Author Only Title Only Author and Title

Zwack PJ, Rashotte AM (2015) Interactions between cytokinin signalling and abiotic stress responses. J Exp Bot 66: 4863–4871
Google Scholar: Author Only Title Only Author and Title